UNCLASSIFIED

AD 292 335

Reproduced
by the

ARMED SERVICES TECHNICAL INFORMATION AGENCY
ARLINGTON HALL STATION
ARLINGTON 12, VIRGINIA
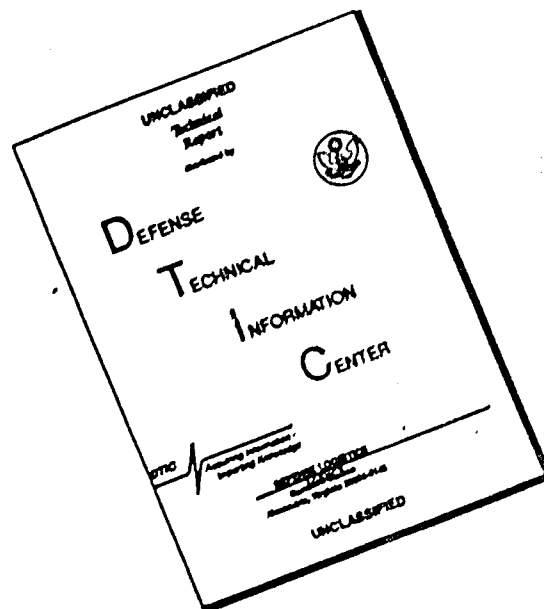
UNCLASSIFIED

DISCLAIMER NOTICE

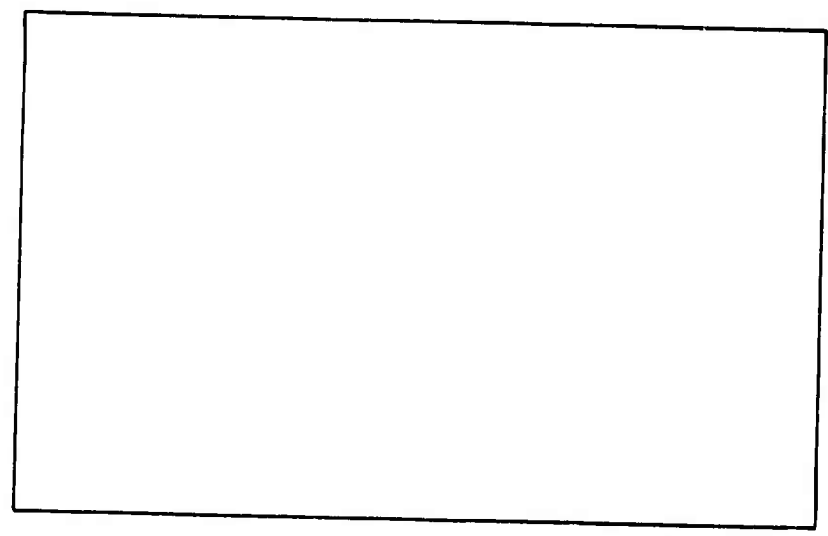THIS DOCUMENT IS BEST QUALITY AVAILABLE. THE COPY FURNISHED TO DTIC CONTAINED A SIGNIFICANT NUMBER OF PAGES WHICH DO NOT REPRODUCE LEGIBLY.

AIR FORCE INSTITUTE OF TECHNOLOGY

AIR UNIVERSITY
UNITED STATES AIR FORCE

SCHOOL OF ENGINEERING

WRIGHT—PATTERSON AIR FORCE BASE, OHIO

EFFECT OF VIBRATION ON
HEAT TRANSFER FROM
CYLINDERS IN FREE CONVECTION

GA/ME/62-4   Robert M. Russ

EFFECT OF VIBRATION ON HEAT TRANSFER

FROM CYLINDERS IN FREE CONVECTION

THESIS

Presented to the Faculty of the School of Engineering of

the Air Force Institute of Technology

Air University

in Partial Fulfillment of the

Requirements for the Degree of

Master of Science

By

Robert M. Russ, B.A.E.

1/Lt   USAF

Graduate Astronautics

August 1962

Preface

The purpose of this study was to investigate a small region in heat transfer. In addition to obtaining the results outlined on the following pages, considerable experience was gained in the fields of instrumentation, research, and technical reporting. However, it should be noted that the areas in description of equipment and analysis of preliminary studies and calculations are too detailed for the majority of readers. These detailed descriptions were included to aid anyone in extending this investigation, and only the general sections of the above need be read.

I wish to express my appreciation to the entire Mechanical Engineering Department for their assistance and interest in this investigation. I wish to express special appreciation to Professor Milton E. Franke, thesis advisor; Dr. Andrew J. Shine, head of the department; and Mr. William Baker and Mr. Frank Jarvis, lab technicans. Special appreciation is extended to Captain Richard W. Hilland for his assistance in obtaining the interferographs for this study. I also wish to express my appreciation to my wife, Carol, for her patience, encouragement, and help in preparing this manuscript; to my children, who were forced to silence without understanding.

Robert M. Russ

Table of Contents

GA/ME/62-4

GA/ME/62-4

List of Figures

GA/ME/62-4

List of Symbols

A   Lateral surface area of test cylinder - in.^2

A_c Cross section area of support rod - in.^2

E   Voltage across circuit - volts

Gr   Grashof number - $(d^3 \beta \rho^2 g \Delta T / \mu^2)_f$ dimensionless

H   Double amplitude of vibration - in.

I   Current throughout circuit - amperes

I_v Vibration intensity - (af) cyc./sec. $\cdot$ in.

L   Length of test cylinder - in.

Nu_s Static Nusselt number - dimensionless

Nu_v Vibrational Nusselt number - dimensionless

Pr   Prandlt number - $(c_p \mu / k)_f$ dimensionless

Q_C Heat loss due to convection - watts

Q_D Heat loss due to conduction - watts

Q_L Heat loss in lead wires - watts

Q_M Heat loss in meters - watts

Q_R Heat loss due to radiation - watts

Q_T Total power in circuit - watts

R   Resistance - ohms

Re   Reynolds number - (vd/ν) dimensionless

Re_v Reynolds number of vibration - $(4afd/144\nu_f)$ dimensionless

T_a Ambient temperature - $^\circ F$

T_{ra} Ambient temperature - $^\circ R$

T_{rw} Surface temperature of cylinder - $^\circ R$

T_w Surface temperature of cylinder - $^\circ F$

a   Amplitude of vibration - in.

c_p Specfic heat of air based on an average temperature between the surface of the cylinder and the ambient environment - BTU/lbm ^{o}F

d Diameter of test cylinder - in.

f Frequency of vibration - cyc./sec.

h Heat transfer coefficient - BTU/hr ft^2 ^{o}F

k Thermal conductivity - BTU/hr ft ^{o}F

k_f Thermal conductivity of air based on an average temperature between the surface of the cylinder and the ambient environment - BTU/hr ft ^{o}F

v Velocity - ft/sec.

β Coefficient of volumetric expansion - ^{o}R^{-1}

ΔT Temperature difference between the surface of the cylinder and the ambient environment - ^{o}F

$\Delta \theta$ Temperature difference between two thermocouples located on the surface of a support rod to determine conduction losses - ^{o}F

ϵ Emissivity - dimensionless

μ_f Dynamic viscosity of air based on an average temperature between the surface of the cylinder and the ambient environment - lbm/sec ft

ν_f Kinematic viscosity of air based on an average temperature between the surface of the cylinder and the ambient environment - ft^2/sec

ρ_f Density of air based on an average temperature between the surface of the cylinder and the ambient environment - lbm/ft^3

σ Stefan-Boltzman constant - 0.1713 x 10^{-8} BTU/ft^2 hr ^{o}R

GA/ME/62-4

Abstract

A number of investigations have been conducted with horizontal cylinders in free convection to determine the effect of vibration on the heat transfer rate. This study was a continuation using higher vibration intensities (product of amplitude and frequency). Also, an attempt was made to correlate the changes in the heat transfer rate with that of forced convection.

The investigation was conducted with three different size cylinders vibrated transversely in air. The diameters of the cylinders were $3/4$, $1/4$, and 0.085 inches. The investigation was conducted over a frequency range of 0 to 130 cps, and an amplitude range of 0 to 0.165 inches. The surface temperature of the cylinders was varied over a range of 125 to 167 $^{\circ}$F.

Results showed that the effect of vibration on the heat transfer rate for a particular cylinder is a function only of the vibration intensity, and that the heat transfer rate is increased over 300% at high vibration intensities. Also, from an interferometer study, the boundary layer is quite complex and goes through several transitions as the vibration intensity is increased. The boundary layer does appear similar to that of forced convection at vibration intensities in excess of 12 inches/second.

ix

EFFECT OF VIBRATION ON HEAT TRANSFER

FROM CYLINDERS IN FREE CONVECTION

GA/ME/62-4

I.   Introduction

Purpose of the Investigation

Because of the presence of vibration in missile and
space systems, it has become essential to understand and
predict the influence of vibration on the heat transfer
rate from various surfaces. It is important to know where
the influence of vibration occurs and to what extent it
occurs. It is also important to understand what mechanisms
are involved.

The purpose of this investigation was to study the
effects of transverse vibrations on the heat transfer rate
from heated horizontal cylinders in free convection. This
purpose entails three objectives: first, to determine the
behavior of the heat transfer rate as vibration intensity
is increased for various diameter cylinders and different
cylinder surface temperatures; second, to observe the boundary
layer of the above phenomenon by means of a Mach-Zehnder
interferometer; third, to establish a correlation between
these results and those of previous investigations.

Past Studies

Heat transfer rates for heated stationary cylinders have
been determined by a number of people, and the results have
been averaged by McAdams with recommended values. McAdams
plotted these values for horizontal cylinders in both free

1

and forced convection where the fluid was passed normal to the cylinder in forced convection (Ref 1:176 & 259). The free convection curve provided a starting point for this investigation. The forced convection curve was used to compare free convection under the influence of vibration with that of forced convection.

In 1957, Shine conducted an investigation into the effects of transverse vibration on the heat transfer rate from a heated vertical plate. He concluded that: (1) the vibration intensity (product of amplitude and frequency) had little or no effect on the heat transfer rate below 1 in./sec.; (2) no relationship existed between the heat transfer coefficient and the position of the heated plate in its cycle; (3) the product of vibration intensity was a useful parameter in describing the effect of vibration on the heat transfer rate; (4) there was no orderly variation in the boundary layer thickness as the plate vibrated (Ref 2:56).

Teleki conducted an investigation of the influence of mechanical vibration on the rate of heat transfer from a horizontal cylinder. He concluded that: (1) the heat transfer coefficient increased as much as 200% with intense vibration; (2) the increase was a function of only one parameter, namely, the pro₍ ct of amplitude and frequency (Ref 3:39).

In 1960, Eisele conducted a study of free convection heat transfer from vibrating cylinders. He determined that: (1) the increase in the heat transfer coefficient was a functio only of the vibration intensity; (2) waviness in the boundary

2

layer occurred only at vibration intensities considerably
higher than the amplitude-frequency product at which a
noticeable change in the heat transfer rate was first observed;
(3) for small tubes and wires vibrating at intensities greater
than 3.5 in./sec., the boundary layer stretches to enclose
the vibratory motion (Ref 4:26).

James, in 1961, investigated vibration intensities up
to 7 in./sec. James concluded that: (1) the diameter of the
cylinder influences the per cent increase in the heat transfer
rate; (2) the temperature difference also influences the heat
transfer rate; (3) the effect of temperature difference
decreased as the vibration intensity increased (Ref 5:17).

In 1961, an investigation was made by Deaver and associates
to determine the effect of low frequency oscillations of
relatively large amplitudes on the heat transfer rate from
a small horizontal wire to water. The conclusions were:
(1) as the Reynolds number of vibration was increased the
corresponding Nusselt number was independent of the Grashof-
Prandtl number; (2) three regions existed of free, mixed, and
forced convection; (3) these regions can be expressed by
empirical equations; (4) at high vibrations the effect of
vibration on the heat transfer rate agreed well with that
of forced convection (Ref 6:4).

Present Study

This study was undertaken to extend and correlate the
preceding investigations. Three different size cylinders

3

of diameters 3/4, 1/4, and 0.085 inches were heated and vibrated transversely in air. The heat transfer coefficients were obtained by experimentally measuring the heat loss through convection. These parameters were converted into Nusselt numbers and plotted against corresponding Reynolds numbers of vibration. The experimental values obtained along with the interferographs were then used to explain and predict the influence of vibration on the heat transfer rate.

II. Description of Equipment

The experimental test apparatus consisted of three test
cylinders, an interferometer, a zirconium light source and a
spark light source, a camera, a resonant beam assembly, a
power control panel, and various measuring devices. An over-
head view of the test area, test cylinder, and various equip-
ment is shown in Figure 1.

The Test Cylinders

Three test cylinders 10 inches long with diameters of
3/4, 1/4, and 0.085 inches were used. The two larger cylinders
were made from 24-ST aluminum, and the 0.085 inch cylinder was
made of stainless steel.

The 3/4 inch Cylinder. The 3/4 inch test cylinder was
manufactured to accommodate an electric heater, thermocouples,
and support rods. The cylinder, shown in Figure 2, had a
machined and polished surface. A 5/16 inch hole was drilled
through the entire length to provide space for the electric
heater.

The heater consisted of 14 feet of #30 gauge nichrome
wire wrapped around a 10 inch long ceramic tube. Sauerisen
cement, with low electrical conductivity, but a high thermal
conductivity, was used to insulate the heater from the cylinder.
The nichrome wire was connected to 16 strands of #30 AWG
copper cable.. The cable was connected to two Powerstats which
controlled the voltage and current supplied to the heater.

Two iron-constantan thermocouples were mounted in two

5
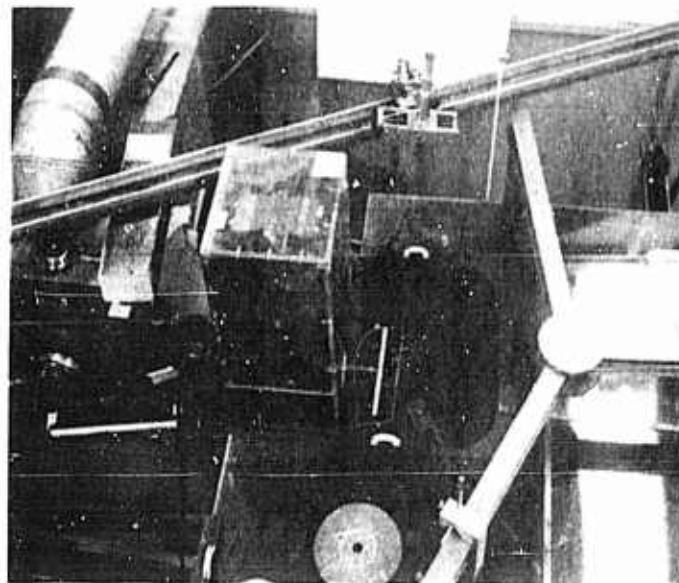
OVERHEAD VIEW OF TEST AREA

FIGURE 1
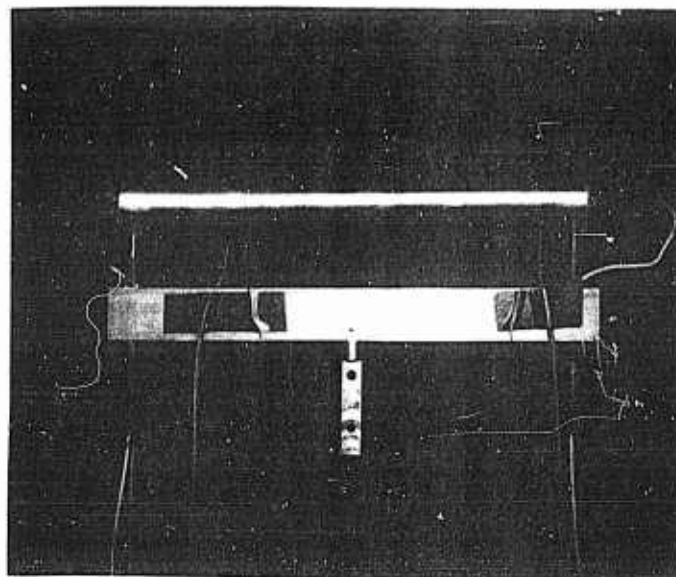
3/4 inch TEST CYLINDER

FIGURE 2

holes drilled radially in the cylinder. The thermocouple leads entered the cylinder through holes drilled axially in both ends, then passed into the radial holes where the junctions were located. The position of these thermocouples is shown in Figures 26 and 27.

Allen screws, as shown in Figures 26 and 27, provided a means of changing the position of the cylinder in the test area. This was necessary so that accurate alignment of the cylinder with the interferometer could be obtained without moving the interferometer.

During the investigation the Sauerisen cement failed to provide a firm attachment between the inner cylinder wall and the heater. This failure resulted in rotational and longitudinal movement of the heater, thus producing fatigue failure of the heater. The movement of the heater element was eliminated by placing caps on each end of the cylinder. The caps were made from phenolic which reduced the heat transfer from the ends of the cylinder.

Figures 26 and 27 of Appendix C show an assembly drawing and parts breakdown drawing of the 3/4 inch test cylinder.

The 1/4 inch Cylinder. The 1/4 inch test cylinder was manufactured to accommodate a single heater wire, external thermocouples, and support rods. This cylinder is shown in Figure 3 and it had a machined and polished surface. A 1/8 inch hole was drilled through the length of the cylinder to provide space for an insulated heater.

7
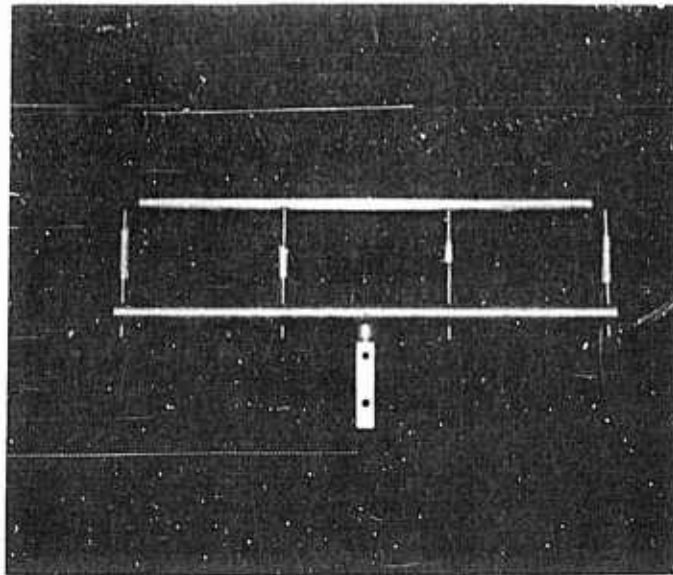
1/4 inch TEST CYLINDER

FIGURE 3

The heater consisted of 10 inches of #30 gauge nichrome wire which was placed inside a 1/8 inch ceramic tube. Copper lead wires were brought through the phenolic end caps and silver soldered to the nichrome wire. The copper lead wires were connected to the Powerstats to provide current and voltage to the single wire heater.

End caps were used to minimize the heat transfer from the ends of the cylinder and to provide support for the copper lead cables. The two interior support rods were used to prevent the thin walled cylinder from rotating and establishing separate modes of vibration between the ends of the cylinder.

Iron-constantan thermocouples were positioned as shown in Figure 3 to measure the cylinder wall temperature. Allen screws provided a means of adjusting the position of

8

the cylinder with respect to the interferometer, so that an accurate alignment could be made without moving the interferometer.

Figures 28 and 29 of Appendix C show an assembly drawing and parts breakdown drawing of the 1/4 inch test cylinder.

The 0.085 inch Cylinder. The 0.085 inch cylinder shown in Figures 4, 30, and 31 was constructed so that the cylinder itself was the heater when current was passed through it.
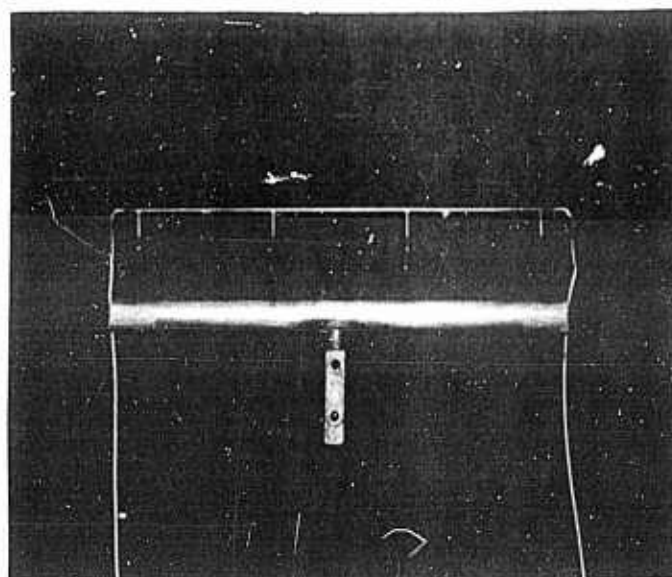
0.085 inch TEST CYLINDER

FIGURE 4

The electric lead wires were silver soldered on the ends of the stainless steel cylinder.

Four small stainless steel rods were soldered on the cylinder to act as support rods. The two interior rods prevented the cylinder from establishing undesirable modes of vibration between the ends of the cylinder.

9

Thermocouples were mounted on the exterior surface by soldering the junction points to the surface of the cylinder. Allen screws, as shown in Figures 30 and 31 provided a means of alignment of the cylinder with the interferometer.

Power Control Panel

The power control panel is shown in Figure 5. Two Powerstat voltage regulators type-140 were used to control the power to the heater of the cylinders. One Powerstat
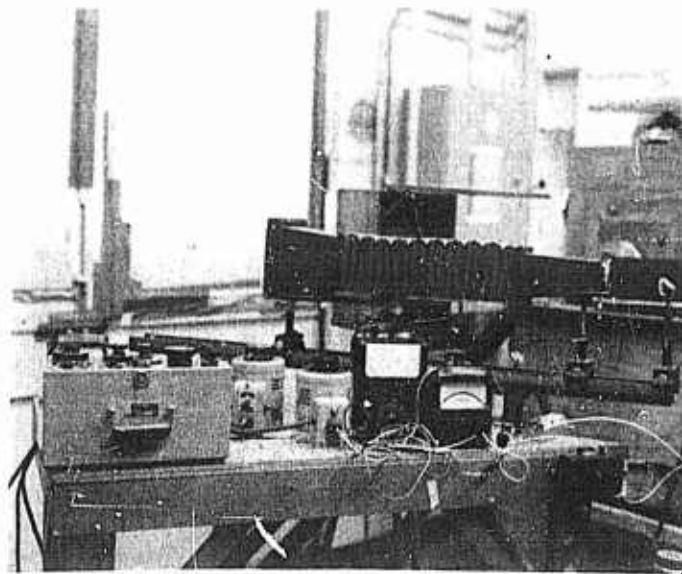
POWER CONTROL PANEL—POTENTIOMETER—CAMERA

FIGURE 5

provided a coarse adjustment of the power, while the other provided a fine adjustment. Three type 20-135 cps Westinghouse voltmeters and three type 20-135 cps Westinghouse ammeters were used to measure the voltage and current in the circuit. A voltmeter with a range of 0 to 30 volts and an ammeter range of 0 to 1 ampere was used in the 3/4 inch cylinder study.

10

For the 1/4 inch cylinder the voltmeter range was from 0 to 20 volts and the ammeter range from 0 to 2 amperes. The small 0.085 inch cylinder required a voltmeter range from 0 to 2 volts and a ammeter range from 0 to 5 amperes.

Temperature Measurement

A Leeds and Northrup potentiometer was used to measure the temperature of the surface of the cylinder. The instrument could read to 0.005 millivolts or approximately 1/3 of a $^{\circ}F$. An ice bath was provided for the thermocouples so that the measurement was based on a 32 $^{\circ}F$ reference.

Vibration Apparatus

General. The primary apparatus used in vibrating the various cylinders was a vibrator excitor power supply, a vibrator motor, and a resonant beam assembly. These items are shown in Figure 6.
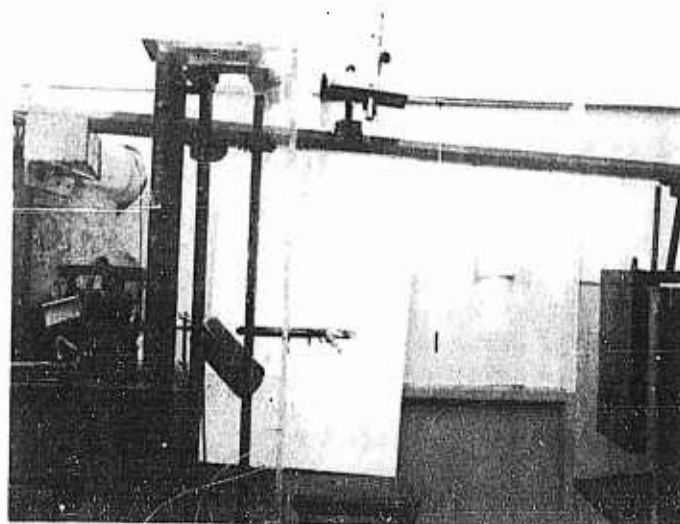
RESONANT BEAM-VIBRATOR MOTOR-TELEMICROSCOPE

FIGURE 6

The natural frequency of the resonant beam was controlled by moving two spacers an equal distance between two 1/2 by 4 inch parallel steel bars, 40 inches long and spaced four inches apart. The natural frequency of the beam was found by changing the frequency on the vibrator excitor power supply until resonance occurred. The amplitude of vibration was controlled by adjusting the power supplied to the vibrator excitor. Two vibrator excitors were employed. The second excitor was used to extend the range of the vibration intensity.

Frequency Measurement. The frequency of the vibrator excitor power supply was controlled by adjusting a dial on the excitor power supply panel. The frequency was checked periodically with a strobotac.

Amplitude Measurement. A Gaertner Scientific Corporation Telemicroscope was used to measure the amplitude of vibration. The telemicroscope was mounted on a transversing mechanism as shown in Figure 6. The amplitude could be read to within a thousandth of an inch.

Boundary Layer Apparatus

Mach-Zehnder Interferometer. The interferometer used in this study is depicted schematically in Figure 25 of Appendix C, and is shown in Figure 7. The test section of the interferometer was 19 inches long and the optical parts were 6 inches in diameter. It was suspended by three coil springs from a steel frame which was supported by a hydraulic jack. The jack, mounted on three wheels, provided mobility and
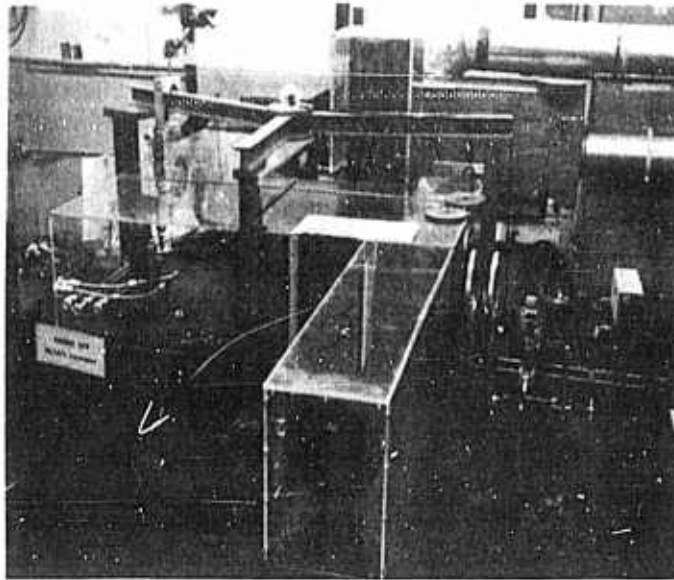
INTERFEROMETER & LIGHT SOURCES

FIGURE 7

height adjustment. The springs allowed leveling of the instrument, and also damped out vibrations. The entire optical system was incased in plexiglass.

Light Sources. A zirconium lamp and a spark lamp were used as the light sources in the interferometer study, Figure 7. The zirconium lamp was used to obtain fine adjustment of the interferometer. The spark lamp provided the light to photograph the instantaneous boundary layer during vibration.

Camera. A Graflex camera, employing type 44 polariod film, was used to record the interferographs. Figure 25 shows schematically the location of the camera, while Figure 5 is a photograph of the camera assembly.

III. Experimental Procedure

General Vibratory Procedure

In all, 54 vibration tests were conducted to determine
the heat transfer rate from the test cylinders. Each test
consisted of one to fifteen runs, or data points. One power
setting was used for each test. Tests were made at three
different settings for each cylinder. The power setting
that was chosen corresponded to ΔT increments of 50, 70, and
90 ^{O}F.. These ΔT values were for the non-vibratory condition
which was the starting point in each test. As soon as the
temperature of the surface of the cylinder became constant
the static data were recorded and the vibratory runs begun.

The frequency during any one test was held constant.
Between the different tests the frequency was varied from
55 cps to 130 cps. The frequency which provided the largest
vibration intensity was found to be 115 cps for the small
vibration excitor and 84 cps for the larger excitor. The
frequency as set on the power excitor panel was checked
periodically with a strobotac and found to agree within 3 cps
of the strobotac reading. The error between the two was less
than 4%.

The amplitude was varied between each run by adjusting
the power supplied to the resonant beam excitor. The amplitude
was measured by means of a telemicroscope. A small line on
the cylinder assembly which reflected light was sighted
through the telemicroscope. This small line was perpendicular

14

to the direction of motion. When the cylinders were subjected to vibration, this line became a bright, distinct band whose width equalled the double amplitude of vibration. Four readings of the width of the band were recorded and the average value used. Small corrections to the double amplitude were made to account for the width of the line. The maximum deviation from the average was 0.01 inches and resulted in an error of less than 8%.

In order to make an accurate comparison of runs, the total power was held constant during any one test. This permitted a comparison of runs, regardless of conditions, with minimum error. Slight variations in the total power between similiar tests were recorded, but these variations were within 4% of each other. The following data were recorded for each run:

1. Ambient temperature of test environment

2. Voltage across system

3. Current in circuit

4. Temperature of the surface of the cylinder

5. Frequency of vibration

6. Double amplitude of vibration

Specific Vibratory Procedure

3/4 inch Cylinder. The cylinder surface temperature required such long periods to stabilize that difficulty was encountered in obtaining data points. This long period of stabilization was primarily caused by the large energy capacity due to the thickness of the cylinder wall. This

prolonged period produced fatigue failure of heaters, thermo-
couples, and vibration apparatus at high vibration intensities.
No method was developed to obtain experimental data at
vibration intensities above 8.5 inches/second. The surface
temperature for the thick walled cylinder was constant along
the cylinder surface. Thermocouple readings for two positions
on the cylinder were within 1/3 $^{\circ}$F of each other.

1/4 inch Cylinder. The stabilization time for the 1/4
inch cylinder was less than 7 minutes for any particular
vibration intensity. This permitted an investigation within
the limits of the vibration apparatus. The surface temperature
of the 1/4 inch cylinder varied up to 3 $^{\circ}$F over the entire
length. An average value of four thermocouples, located at
various positions on the surface, was used as the surface
temperature. One thermocouple was placed near the outside
support rod. Another was positioned near an interior support
rod. The remaining two thermocouples were located in the
center between the support rods.

0.085 inch Cylinder. The stabilization time for the
0.085 inch cylinder was less than 2 minutes. Therefore,
experimental data were easy to obtain. The surface temperature
was found to vary quite significantly over the length of the
cylinder. This variation occurred both statically and during
vibration. A typical profile of the temperature is shown in
Figure 8 for both cases. Nineteen thermocouples were located
along the surface of the cylinder to determine the temperature
distribution. During vibration a number of thermocouples

16
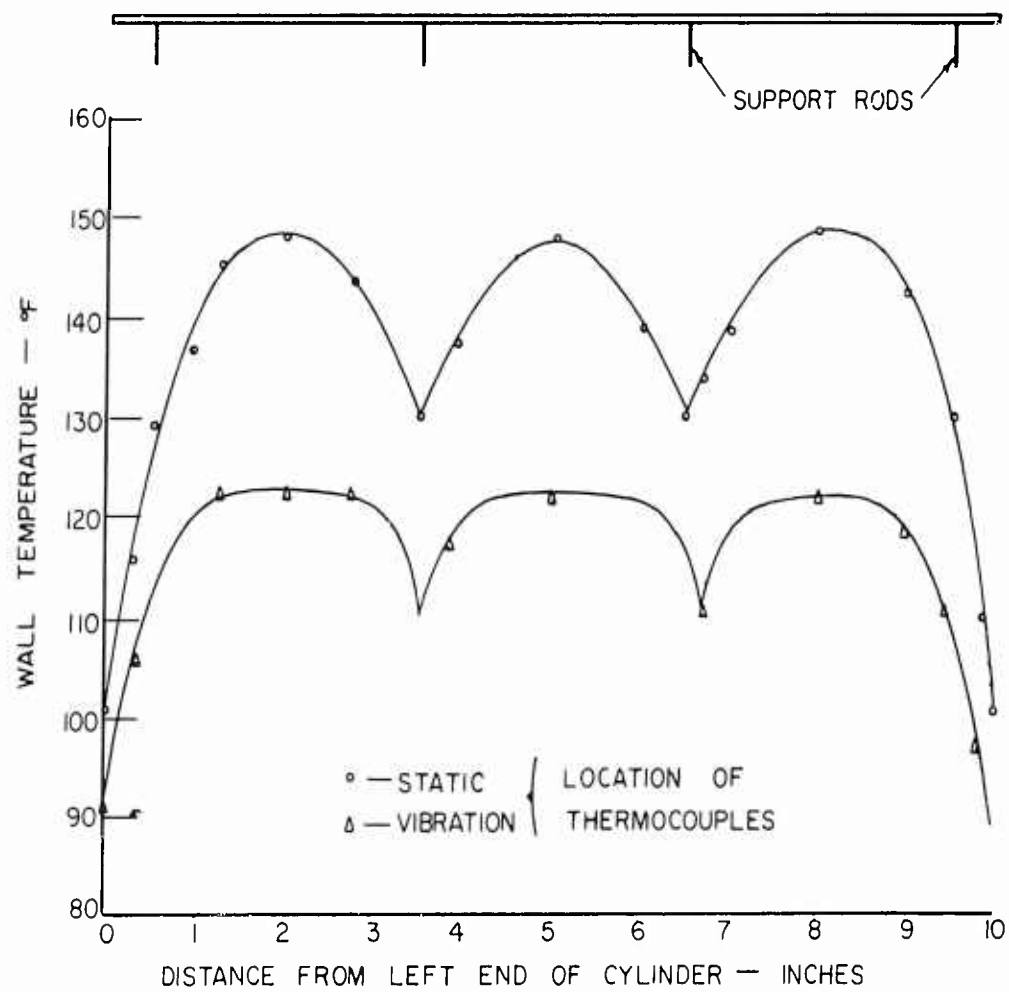
FIGURE 8

failed, and the sufficient number of thermocouples in the static profile suggested a similiar profile in the vibratory case. The average temperature was determined from the profile by computing the area under the curve and dividing this area by the length of the cylinder. In four static and vibration runs, one particular thermocouple reading was the same as the average temperature. This thermocouple was then used as the representative average surface temperature for the remaining tests.

Boundary Layer Procedure

The zirconium lamp was used to provide a constant illumination so that an infinite fringe adjustment of the interferometer could be made. Once vibration had begun and stabilization had been reached, the zirconium lamp was removed and a spark lamp was employed to provide a light that would allow a photograph of the instantaneous boundary layer to be taken. In the majority of cases, the infinite fringe was lost by the above procedure because of the stabilization time. To overcome this problem, the interferographs were taken within 20 seconds after vibration had begun.

The parameters recorded during the boundary layer interferograph investigation were:

1. Voltage across system

2. Current in circuit

3. Frequency of vibration

4. Double amplitude of vibration

The location of the cylinder during vibration was

determined by means of a reference wire, which appears in
each interferograph. The direction of motion of the cylinder
in each interferograph was not determined, but from the
boundary layer the direction could be presumed.

IV. Calculation Procedure

Previous studies revealed that the use of an interferometer to determine the heat transfer rate at high vibration intensities was impractical due to the long stabilization periods involved and a very complex fringe pattern in the boundary layer. Therefore, the heat transfer rate was evaluated by determining the heat loss through convection from the total power in the circuit. This heat loss is found from the equation:

$$Q_C = Q_T - Q_D - Q_R - Q_L - Q_M \tag{1}$$

where the above quantities refer to convection, total, conduction, radiation, lead wires, and meter heat losses respectively.

The total power, Q_T, was determined from the equation:

$$Q_T = EI \tag{2}$$

The conduction losses through the support rods where determined from the equation:

$$Q_D = 0.0334 \, \Delta\theta \tag{3}$$

and

$$Q_D = 0.0128 \, \Delta\theta \tag{4}$$

where equation (3) refers to the 1/4 inch diameter cylinder and (4) to the 0.085 inch cylinder. Complete development of the above equations is contained in Appendix B along with Figures 20 and 21 to determine the values of $\Delta\theta$.

20

The radiation losses were determined from the equation:

$$Q_R = 0.2931\sigma\epsilon A(T_{rw}^4 - T_{ra}^4) \tag{5}$$

Appendix B contains values of the emissivity and the percentage of power loss from radiation. Figures 22, 23, and 24 contain curves to determine the radiation loss directly for the three test cylinders.

The line and meter losses were determined from the equation:

$$Q_L \text{ or } Q_M = I^2R \tag{6}$$

Values of the resistance for each case along with the percentage of the total power are contained in Appendix B under the sections titled "Line Losses" and "Meter Losses".

From Q_C the heat transfer rate, defined in non-dimensional form, was obtained from the equation:

$$Nu_v = hd/k_f = 3.412 \ Q_C/\pi Lk_f\Delta T \tag{7}$$

or for the three cylinders, each 10 inches in length:

$$Nu_v = 1.3 \ Q_C/k_f\Delta T \tag{8}$$

Where 3.412 and 1.3 are conversion factors.

The vibration parameter was defined by the Reynolds number and the vibration intensity equations:

$$Re = vd/\nu \tag{9}$$

and

$$I_v = af \tag{10}$$

21

where the velocity (v) in equation (9) was replaced by the frequency (f) times the total distance traveled (4a) during one cycle. The resulting Reynolds number equation becomes:

$$Re_v = 4afd/144 \, \nu_f \tag{11}$$

where 144 is a conversion factor.

The Nu_v, Re_v, and L_v were the parameters used to present the influence of vibration on the heat transfer rate.

V. Discussion of Results

The experimental data for each run and the values of the Nusselt and Reynolds number of vibration are tabulated in Tables I, II, and III of Appendix E. Figures 9, 10, and 11 contain graphs of the $Nu/Pr^{.3}$ versus Re_v for each test. A sample calculation showing the method of evaluating the Nusselt and Reynolds number of vibration is contained in Appendix D.

Figures 9, 10, 11, and 12 are plotted using a Re_v which is analogous to the vibration intensity. The two terms differ only by constants and the kinematic viscosity which varies only slightly over the temperature range of this investigation. The vibration intensity would shift the curves of Figures 9, 10, 11, and 12 to the left by a constant amount, but the slopes would remain the same. In the remaining portion of this report the vibration intensity is used to explain the influnce of vibration on the heat transfer rate.

Experimental Results

In the investigation, the cylinders were heated to various surface temperatures, and the heat transfer rates for these static conditions were obtained. These values of the heat transfer rate are compared with McAdams recommended curve for free convection which is shown in Figure 19 of Appendix B. In all cases the static values agreed with McAdams within $\pm 10\%$.

The graphs, Figures 9, 10, and 11, of $Nu/Pr^{.3}$ versus Re_v show that the heat transfer rate is increased considerably as

23

FIGURE 9

FIGURE 10

EFFECT OF VIBRATION ON HEAT TRANSFER RATE FOR 0.085" DIAMETER CYLINDER
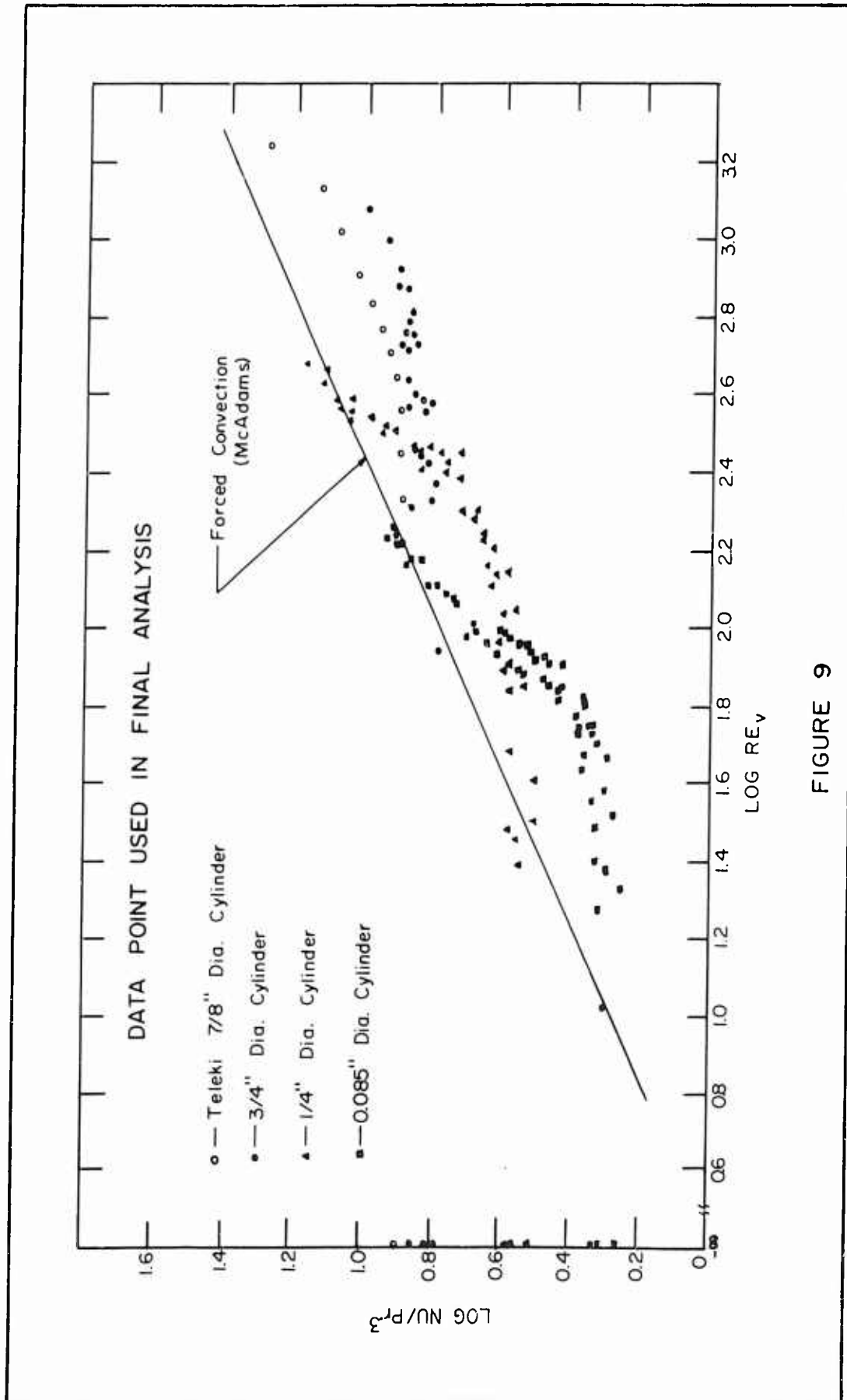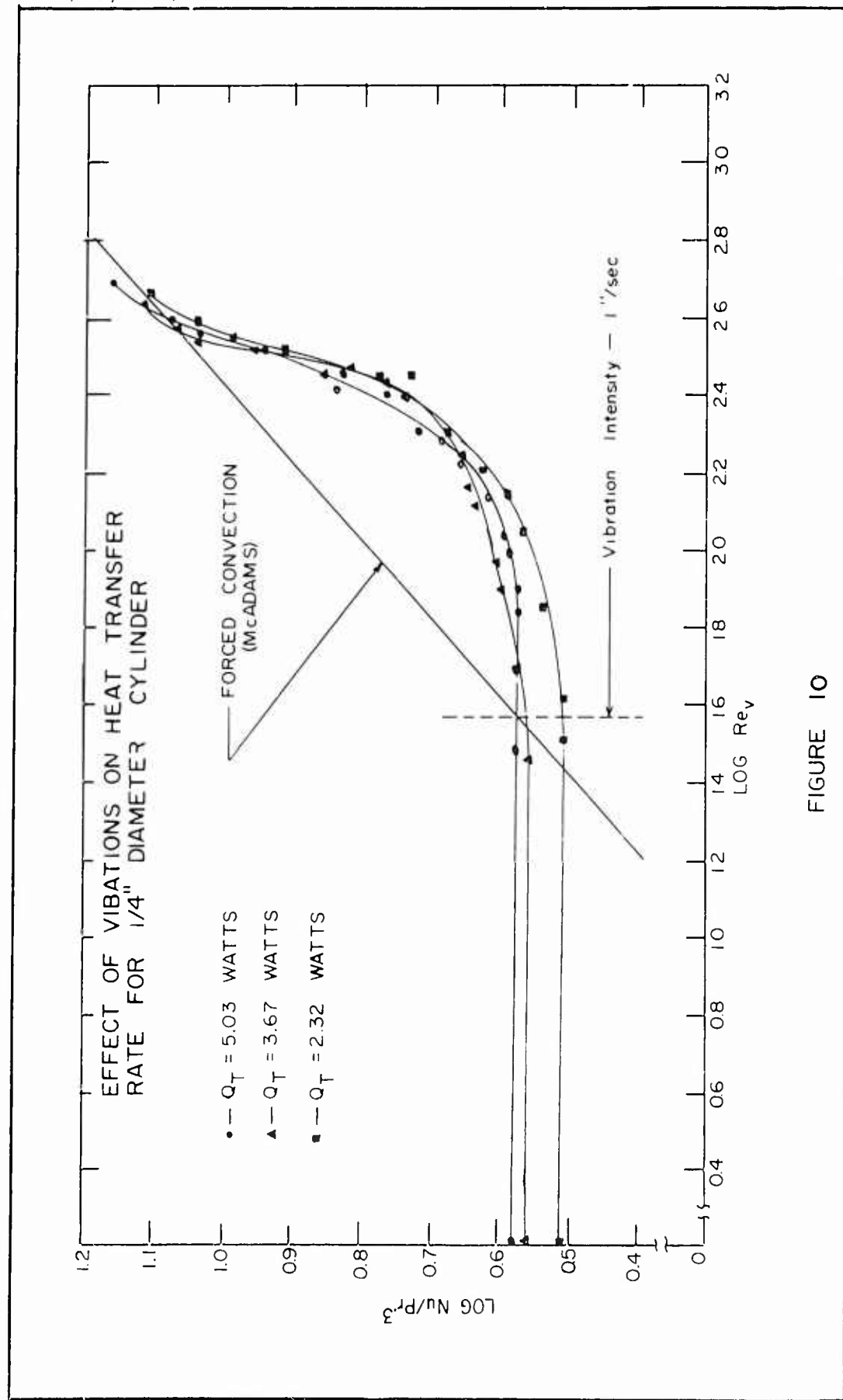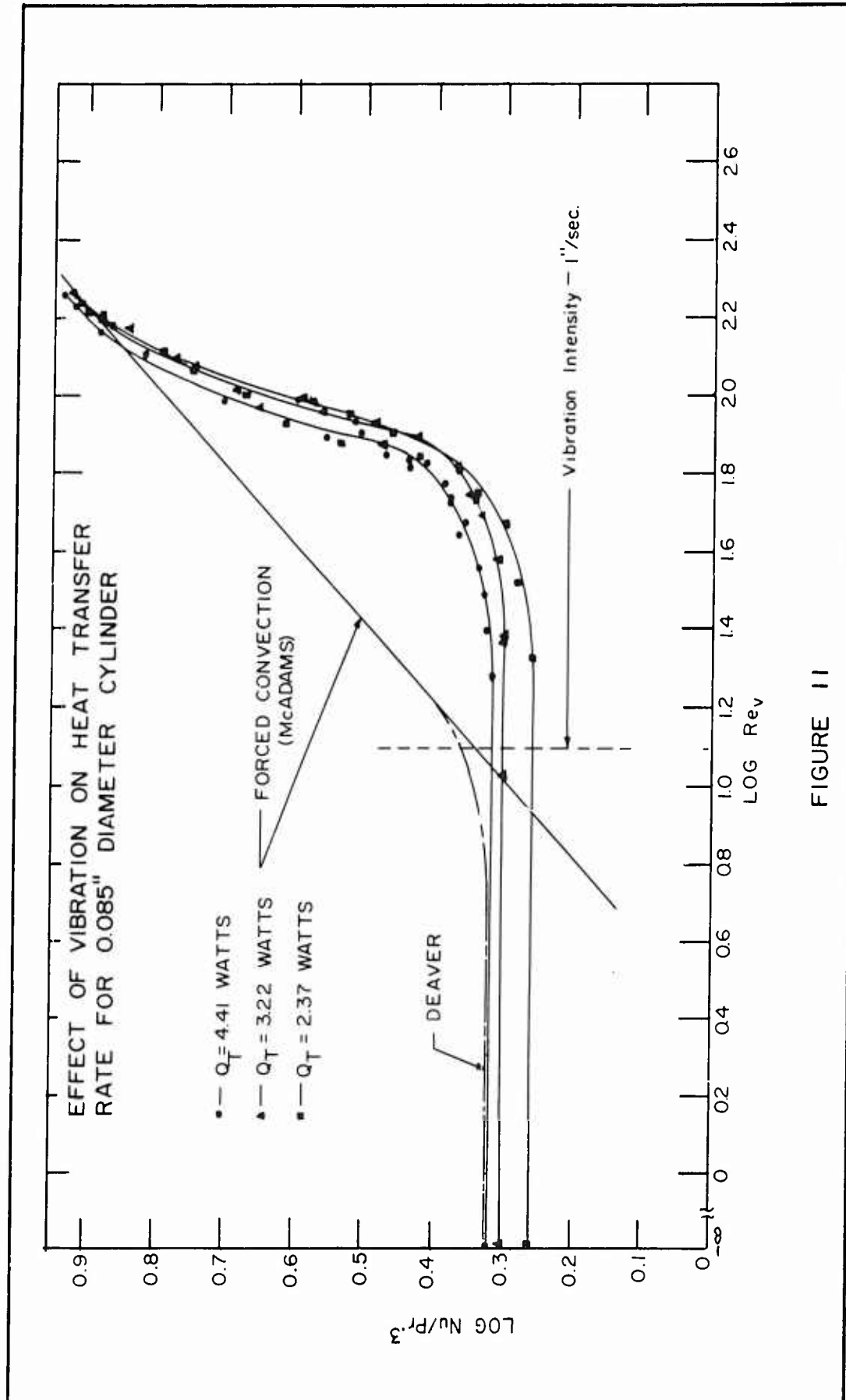
FIGURE II

the vibration intensity is increased. The graphs show a gradual increase in the heat transfer rate after a vibration intensity of 1 in./sec. is exceeded. As the vibration intensity is increased further the change in the slope of the curves becomes relatively constant. Further increase in the vibration intensity past the second breaking point produces a decrease in the slope of the curves.

Effect of Diameter on the Heat Transfer Rate. The diameter size of the cylinder does produce a difference in the heat transfer rate as shown in Figure 9. However, the slope of the curves, Figures 10 and 11, is independent of the diameter. It appears from the curves that if the vibration intensity is increased considerably over the maximum values used in this investigation that the heat transfer rate will become independent of the diameter. This is based on the assumption that the curves will follow that of forced convection.

Effect of Temperature on the Heat Transfer Rate. The increments of temperature difference between the surface of the cylinder and the ambient environment produce a difference in the heat transfer rate as shown in Figures 9, 10, and 11. This difference in the heat transfer rate occurs at the static conditions and low vibration intensities. As the vibration intensity is increased this difference in the heat transfer rate dimishes, and the heat transfer rate becomes independent of the temperature difference above vibration intensities of 7 in./sec.

27

Effect of Vibration Intensity on the Heat Transfer Rate.
The heat transfer rate was found to increase as much as 320%
for the 1/4 inch cylinder and 350% for the 0.085 inch cylinder
at vibration intensities in excess of 12 in./sec. These
percentages were the highest values obtained in this investi-
gation due to the limitations in vibration intensity. From
Figures 9, 10, and 11 it appears that at high vibration
intensities for a particular cylinder, the only parameter
influencing the heat transfer rate is the vibration intensity.

The behavior of the heat transfer rate as the vibration
intensity is increased is shown in Figures 9, 10, and 11.
There appear to be four regions: first, the region where
the heat transfer rate is unaffected by the vibration; second,
a region of transition where the slope of the curves changes
from a zero value to the maximum value; third, a region where
the slope of the curves remains relatively constant; and
fourth, a region where transition occurs again and the slope
of the curves decreases to a smaller constant value. From
the graphs it appears that the curves then tend to follow that
of forced convection. The first transition occurs gradually
as the vibration intensity is increased, while the second
transition occurs more abruptly. No analysis was made to
express the behavior of the heat transfer rate by means of
empirical equations.

Boundary Layer Results

The boundary layer for one particular test is shown in

GA/ME/62-4

Figures 13, 14, 15, and 16. The sequence of interferographs is arranged for increasing vibration intensity. The location of the interferograph with respect to Nusselt and Reynolds number is shown in Figure 12. The per cent increase in the heat transfer rate is shown also in Figures 13, 14, 15, and 16.

Interferographs 1 and 2 show the unaffected region of vibration. The interferographs 3, 4, and 5 depict the first transition region. In 6, 7, 8, 9, 10, and 11 the region where the slope of the curve is a maximum is shown. Interferographs 12, 13, 14, and 15 show the second transition region. While the interferograph 16 shows the boundary layer at the point where the slope of the curve is reduced to a smaller constant value. From the sequence of interferographs it is evident that the mechanisms involved are quite complex. In the first region the boundary layer is relatively undisturbed by the vibration. As the vibration intensity increases the boundary layer is distorted and tends to flatten out, and it is apparent that free convection no longer exists. Further increase in the vibration intensity produces a fanning out of boundary layer with considerable turbulence. In the higher regions of vibration intensity the boundary layer becomes quite thin as in forced convection.

Figures 17 and 18 show the boundary layer for the 3/4 and 0.085 inch cylinder in the lower vibration intensity regions. Values of the Nusselt number ratio are also shown.

29

Correlation

The vibration intensity for a particular cylinder was found to be the only parameter affecting the heat transfer rate as observed by Shine, Teleki, Eisele, and James. Also, the critical vibration intensity, as defined by Shine, occurred at an approximate vibration intensity of 1 inch/sec. as shown in Figures 10 and 11.

Figure 9 shows data points obtained by Teleki with a 7/8 inch diameter cylinder. The general shape of the curve and the values of the points agree with the findings in this investigation. The per cent increase in the heat transfer rate was found to be higher than Teleki observed; but this is attributed to the higher vibration intensities, 15 in./sec. compared to 12 in./sec., used in this investigation.

Agreement with James was obtained with respect to the influence of the temperature increment on the heat transfer rate. At vibration intensities in excess of 7 in./sec. it was found that the temperature increments had little or no effect on the heat transfer rate. James also concluded that the rate of change in the heat transfer increases as smaller diameter cylinders are employed. From Figure 9 it appears that the curves will follow that of forced convection. If this is true, then the heat transfer rate will become independent of the diameter of the cylinder at high vibration intensities.

The findings of Deaver could not be correlated with this investigation. Four regions with complex boundary layers

30

were observed in this investigation, while Deaver observed
only three regions of free, mixed, and forced convection.
Applying the empirical equations of Deaver to the 0.085 inch
diameter cylinder, a smooth transition from free to forced
convection is obtained as shown in Figure 11. The results of
this investigation, as shown in Figure 11, undergo a more
complex transition.

The attempt to correlate the influence of vibration on
the heat transfer rate to that of forced convection proved
unsatisfactory. This is shown in Figures 9, 10, and 11.
However, it appears that at the high vibration intensities,
the effect of vibration does correspond to that of forced
convection, but the extension of the curves could not be
obtained because of the limitations of the vibration apparatus.

VI. Conclusions and Recommendations

The results of this investigation of the effect of transverse vibrations on the heat transfer rate from heated horizontal cylinders in air lead to the following conclusions:

1. The diameter of the cylinder has an appreciable effect on the heat transfer rate.

2. The increments of temperature difference produce no appreciable change in the heat transfer rate at high vibration intensities.

3. The heat transfer rate for a given test cylinder is affected by only the vibration intensity.

4. The increase in the heat transfer rate exceeds 300% at high vibration intensities.

5. The behavior of the heat transfer rate as a function of the vibration intensity is quite complex and no simple analogy to that of forced convection exists for the range of this investigation.

6. The boundary layer changes considerably as the vibration intensity is increased, and approaches that observed in forced convection.

In the design of modern equipment it is important to be able to predict the influence of vibration on the heat transfer rate. It is recommended that even higher regions of vibration intensity be investigated to see if a correlation does exist between vibration and forced convection. Also, an environment

32

other than air should be investigated. The disagreement of this investigation with that of Deaver's might have resulted from the environment or technique used.

It is recommended that the design of the cylinders be similiar to the 1/4 inch diameter cylinder in this investigation or that used by Teleki (Ref 3:9). Also, at high vibration intensities the stabilization time becomes an important factor, and thin walled cylinders should be employed to minimize the stabilization time.

Bibliography

1. McAdams, W.H. Heat Transmission. New York, New York:
   McGraw-Hill Co., Inc. 1954.

2. Shine, A.J. The Effect of Transverse Vibrations on the
   Heat Transfer Rate from a Heated Vertical Plate in Free
   Convection. Technical Report 57-13. Wright-Patterson
   Air Force Base, Ohio: Wright Air Development Center,
   December 1957.

3. Teleki, C. The Influence of Vertical Vibrations on the
   Rate of Heat Transfer from a Horizontal Cylinder in Air.
   Technical Note 59-357. Wright-Patterson Air Force Base,
   Ohio: Wright Air Development Center, October 1960.

4. Eisele, D.F. The Effects of Vibrations on the Heat
   Transfer Rate from Cylinders in Free Convection.
   Thesis (unpublished). Dayton, Ohio: Air Force
   Institute of Technology, August 1960.

5. James, E.C. The Effect of Vibration on the Heat Transfer
   Rate from Cylinders in Free Convection. Thesis (unpublished).
   Dayton, Ohio: Air Force Institute of Technology, August 1961.

6. Deaver, F.K., Penny, W.R., and Jefferson, T.B. Heat
   Transfer from an Oscillating Horizontal Wire to Water.
   ASME Paper No. 61-WA-178, 1961.

7. Eckert, E.R.G. and Drake, R.M. Jr. Heat and Mass Transfer.
   New York, New York: McGraw-Hill Co., Inc. 1959.

8. Pagonis, G.A. The Light Metals Handbook (Text). New York,
   New York: D. Van Nostraud Co., Inc. 1954.

9. Kaybill, E.K. Electric Circuits for Engineers. New York,
   New York: The MacMillan Co. 1951.

APPENDIX A

<u>Interferographs</u>

INTERFEROGRAPHS POSITION
FOR VIBRATING
1/4" DIAMETER CYLINDER

$Q_T = 3.67$ WATTS

FORCED CONVECTION
(McADAMS)

LOG Rev

LOG Nu/Pr.3

FIGURE 12

(1)
STATIC POSITION — CENTER
$Nu_v/Nu_s = 100\%$

(2)
POSITION — RIGHT OF CENTER
$Nu_v/Nu_s = 100\%$

(3)
POSITION — AT CENTER
$Nu_v/Nu_s = 103.5\%$

(4)
POSITION — RIGHT OF CENTER
$Nu_v/Nu_s = 108\%$

FIGURE 13

(5)
POSITION — AT CENTER
$Nu_V/Nu_S = 118\%$

(6)
POSITION — RIGHT OF CENTER
$Nu_V/Nu_S = 125\%$

(7)
POSITION — RIGHT OF CENTER
$Nu_V/Nu_S = 132\%$

(8)
POSITION — LEFT OF CENTER
$Nu_V/Nu_S = 143\%$

FIGURE 14
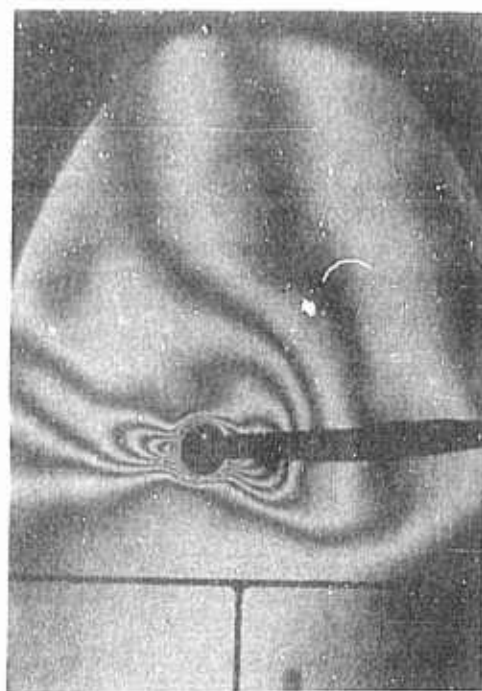
(9)
POSITION — AT CENTER

$Nu_v/Nu_s = 151\%$
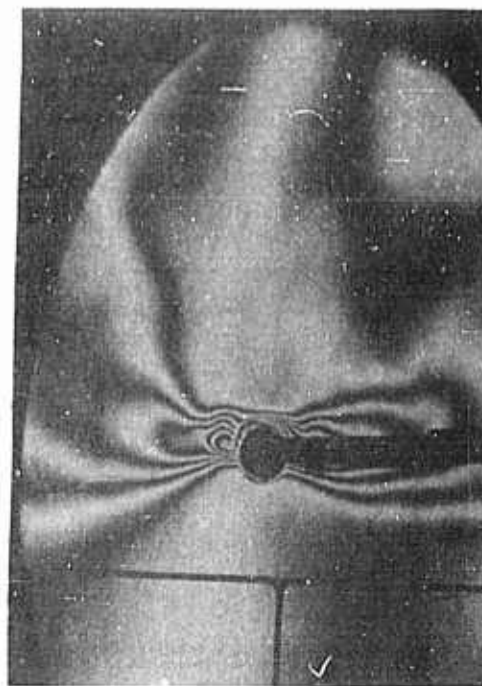
(10)
POSITION — RIGHT OF CENTER

$Nu_v/Nu_s = 164\%$
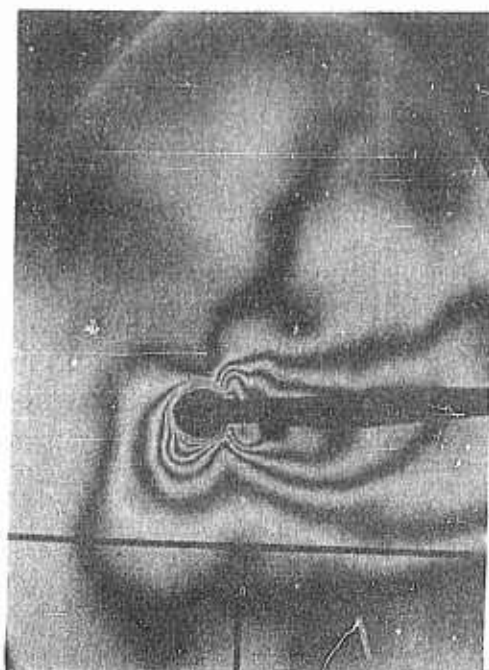
(11)
POSITION — LEFT OF CENTER

$Nu_v/Nu_s = 173\%$
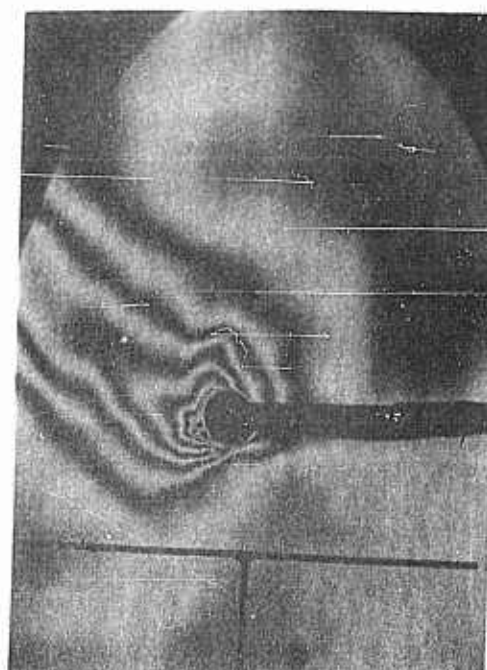
(12)
POSITION — RIGHT OF CENTER

$Nu_v/Nu_s = 186\%$

FIGURE 15
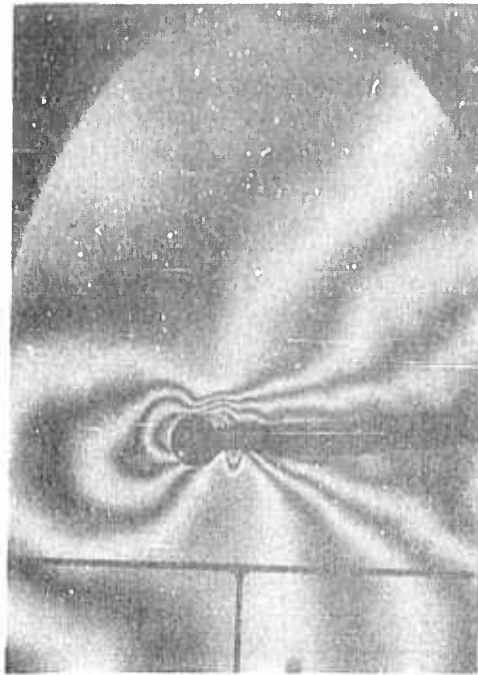
(13)
POSITION — AT CENTER
$Nu_V/Nu_S = 194\%$
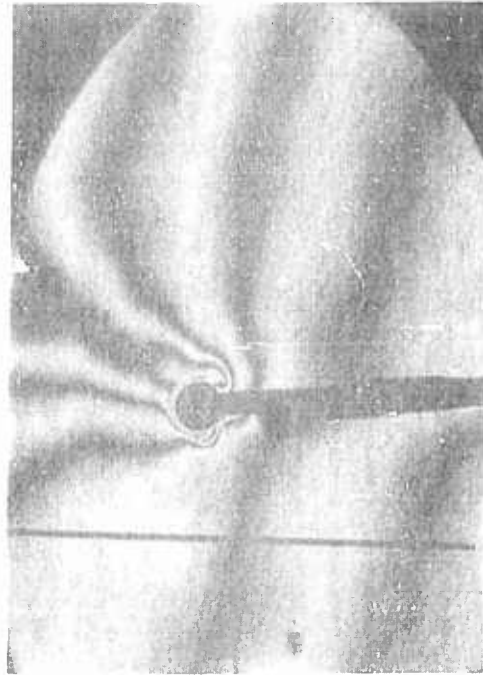
(14)
POSITION — LEFT OF CENTER
$Nu_V/Nu_S = 194\%$
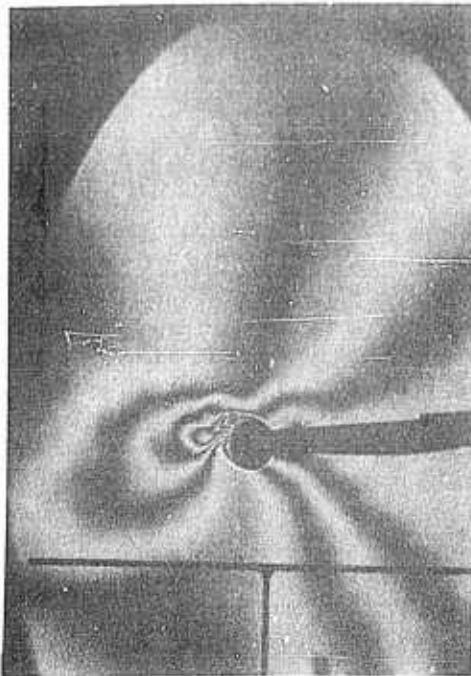
(15)
POSITION — RIGHT OF CENTER
$Nu_V/Nu_S = 199\%$
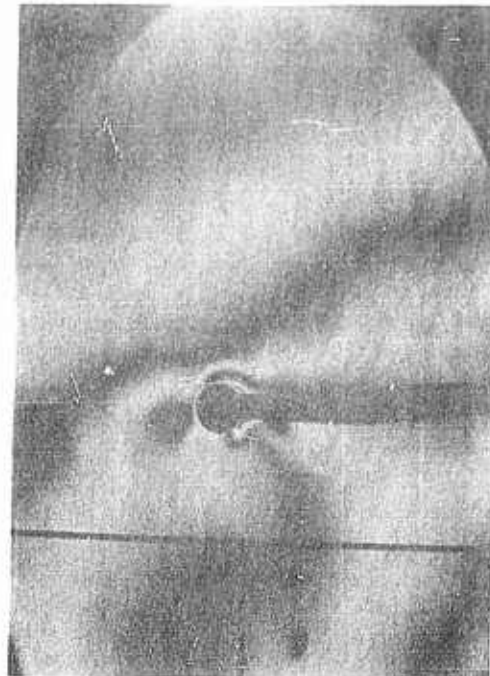
(16)
POSITION — LEFT OF CENTER
$Nu_V/Nu_S = 202\%$

FIGURE 16
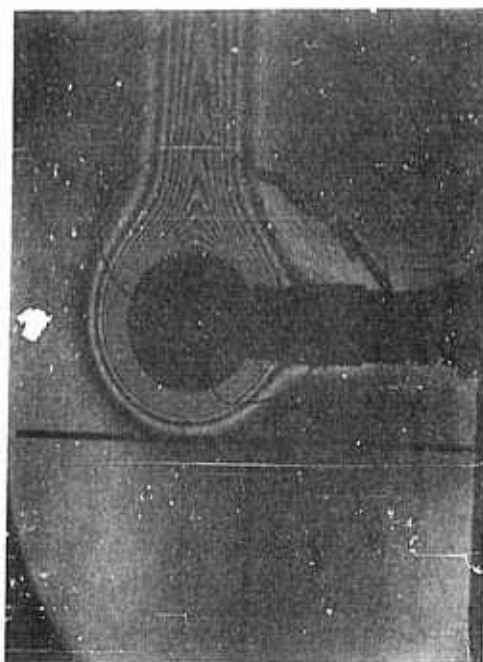
STATIC POSITION — AT CENTER
$Nu_v/Nu_s = 100\%$
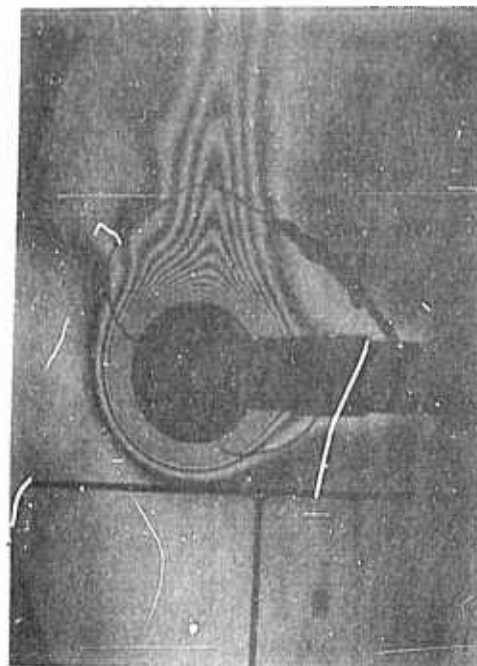
POSITION — LEFT OF CENTER
$Nu_v/Nu_s = 104\%$
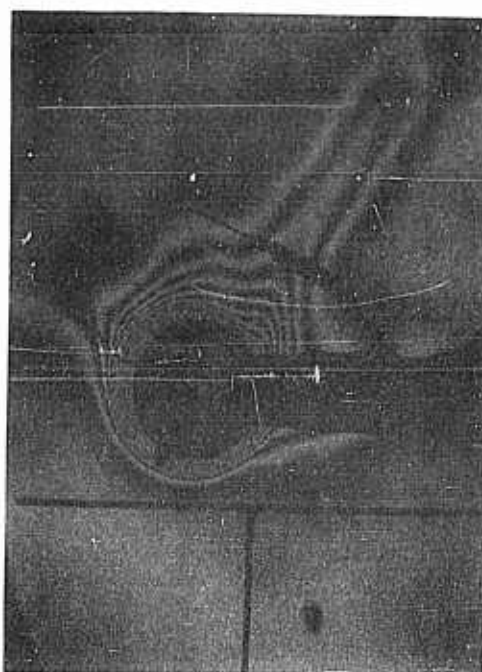
POSITION — RIGHT OF CENTER
$Nu_v/Nu_s = 110\%$
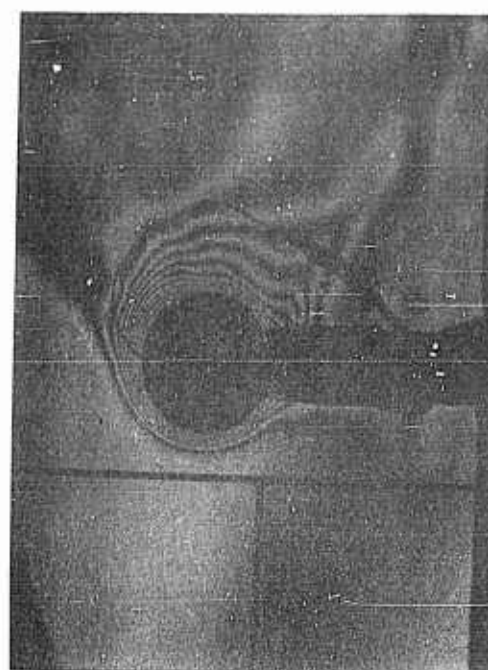
POSITION — RIGHT OF CENTER
$Nu_v/Nu_s = 114\%$
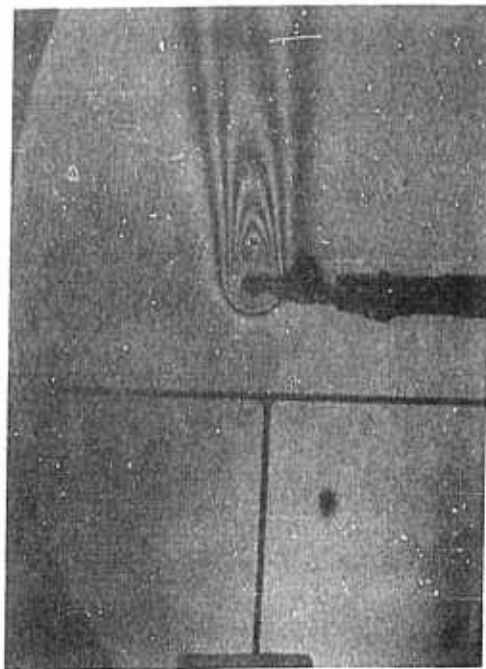
FIGURE 17

STATIC POSITION — AT CENTER
$Nu_V/Nu_S = 100\%$
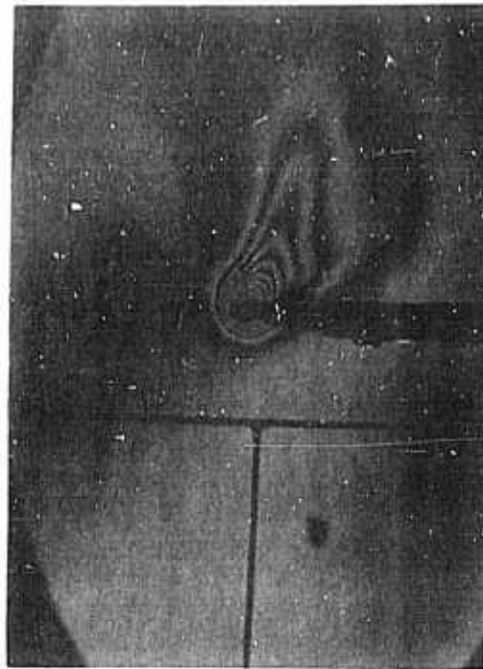
POSITION — LEFT OF CENTER
$Nu_V/Nu_S = 106\%$

POSITION — RIGHT OF CENTER
$Nu_V/Nu_S = 118\%$
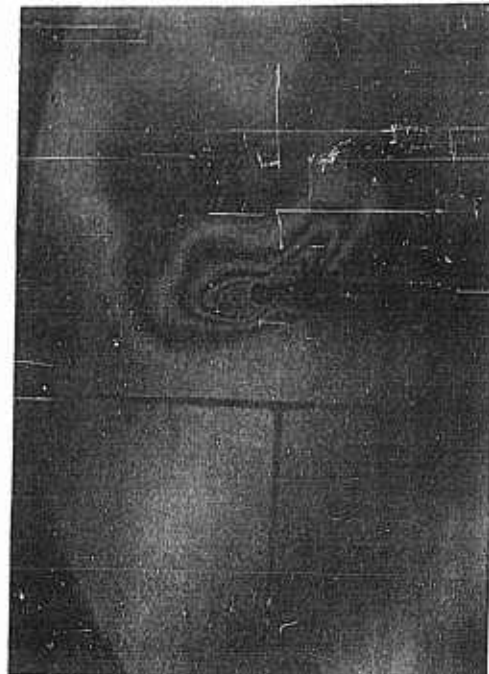
POSITION — LEFT OF CENTER
$Nu_V/Nu_S = 130\%$
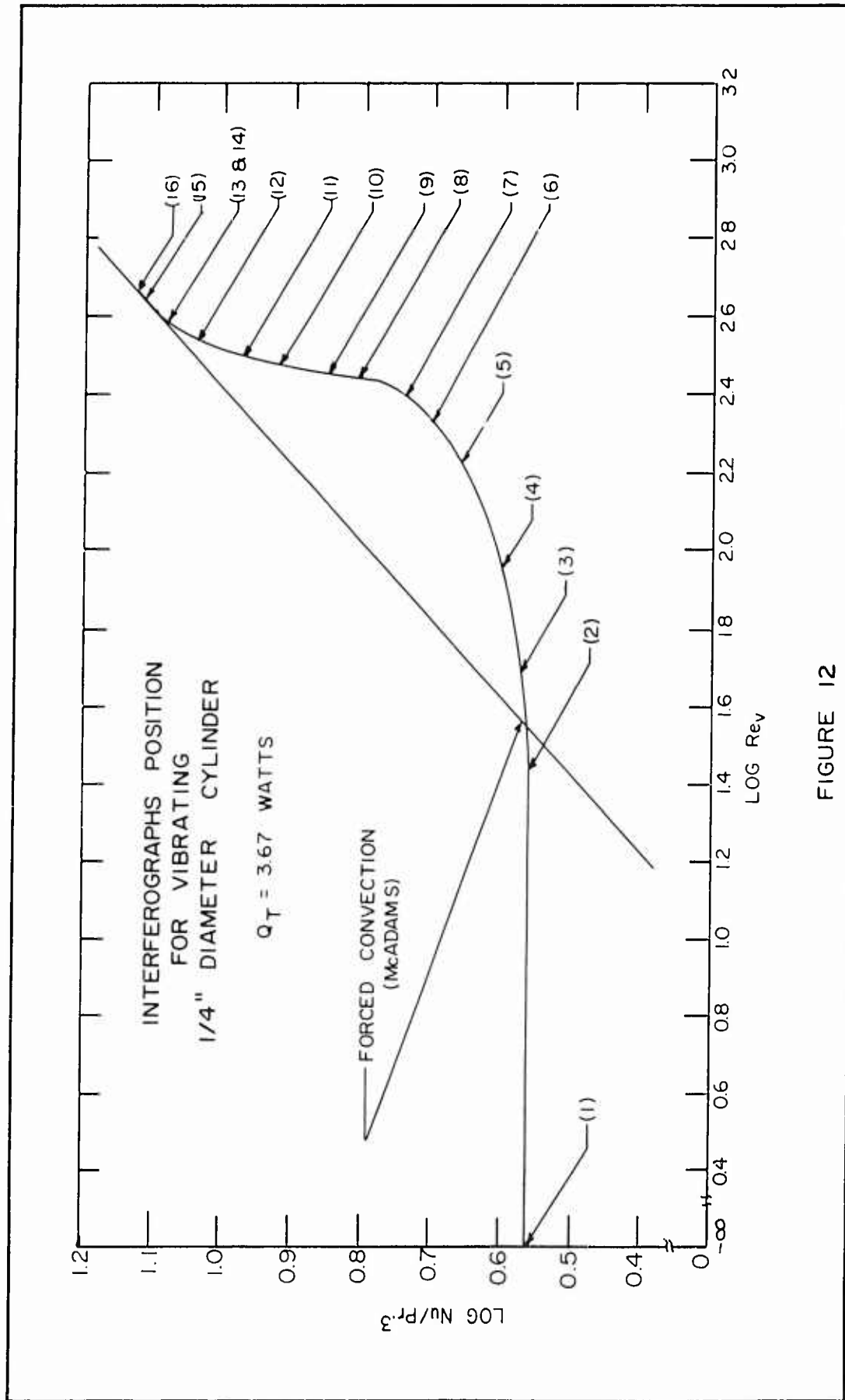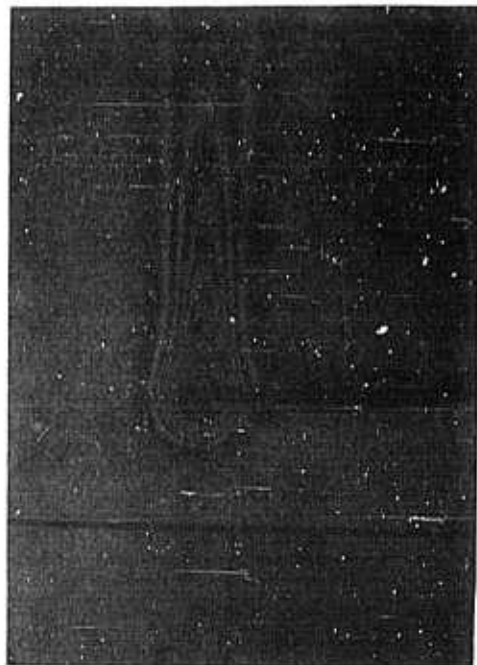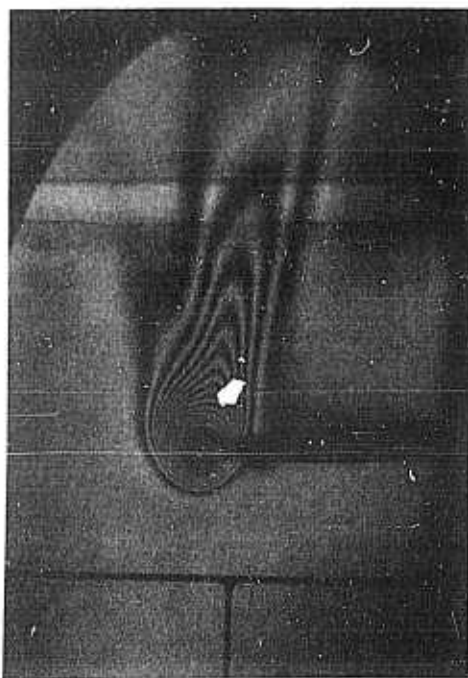
FIGURE 18
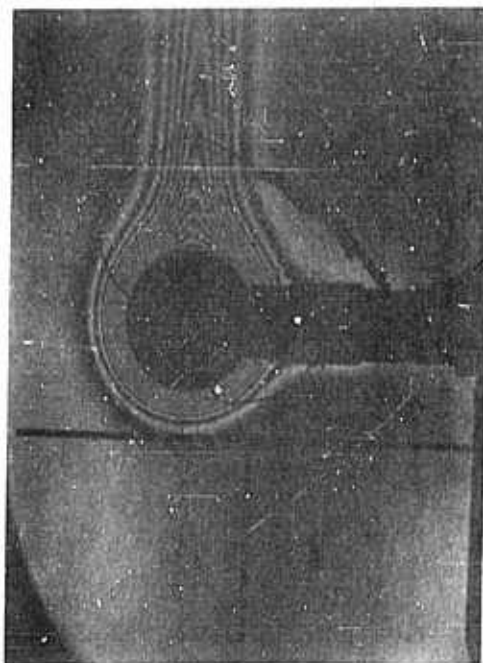
STATIC POSITION — AT CENTER
$Nu_V/Nu_S = 100\%$
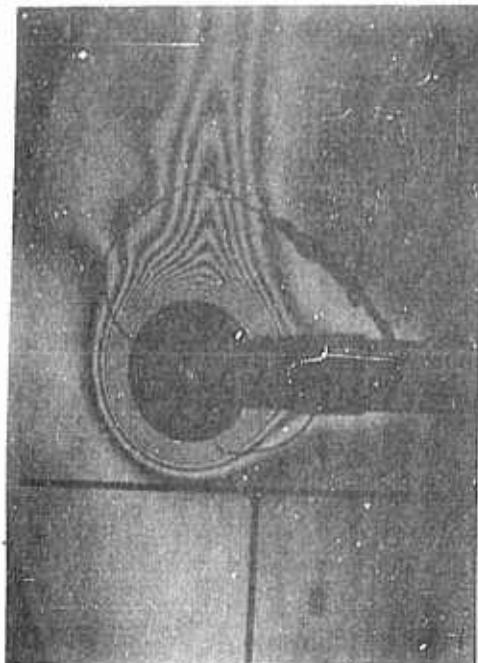
POSITION — LEFT OF CENTER
$Nu_V/Nu_S = 104\%$

POSITION — RIGHT OF CENTER
$Nu_V/Nu_S = 110\%$
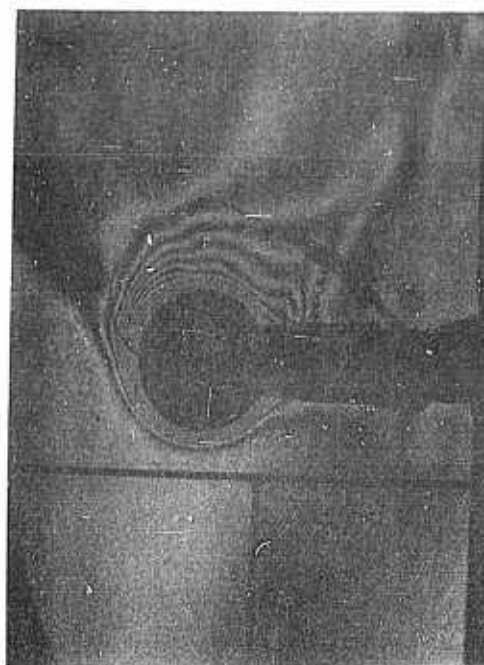
POSITION — RIGHT OF CENTER
$Nu_V/Nu_S = 114\%$

FIGURE 17

APPENDIX B

Analysis of Preliminary

Studies and Calculations

Wire Configuration

From previous work in this area it was found that at high vibration intensities the heater wires and thermocouple wires tend to fail due to fatigue. An investigation was conducted to determine the best size wire, type mount, and type of support necessary to reduce fatigue failure. Different size heater wires, lead cables, and thermocouple wires were mounted in various positions on a cylinder. Saurisen cement, aluminum paste, and silver solder were used to fix the wires to the surface of the cylinder. The cylinder was vibrated at intensities in excess of 7 in./sec. for a period of 45 minutes.

It was found that the smaller diameter heater and thermocouple wires resisted fatigue failure longer than larger diameter wires. Lead cables constructed from 16 to 19 strands of #18 to #20 AWG copper wire were found to resist fatigue failure longer than larger or smaller cables.

The Saurisen cement was found to harden into a brittle compound and break from the surface. Aluminum paste was found to be very satisfactory on the 3/4 and 1/4 inch cylinders. It was found that by soldering the thermocouples on the surface of the small stainless steel cylinder the failure rate was reduced to a negligible quantity.

Securing all wires and cables to the support rod eliminated the oscillation of the entire mass of the wires or cables from acting on the junction points. This is shown in Figures 2, 3, and 4.

44

Static Comparison

Prior to each run, the static values of the heat transfer rate were compared to existing data. The corresponding Nusselt number along with the Grashof-Prandlt number was determined for a ΔT increment and compared to the free convection curve recommended by McAdams. This comparison is shown in Figure 19. In all cases the calculated values agreed closely with McAdams and were within the zone of Nusselt's and Rice's experimental curves.

Static values, in some cases, were computed by means of the interferometer as done by Eisele (Ref 4). The values obtained in this manner were within 10% of those computed by the procedure in this report.

FREE CONVECTION COMPARISON
STATIC CONDITIONS
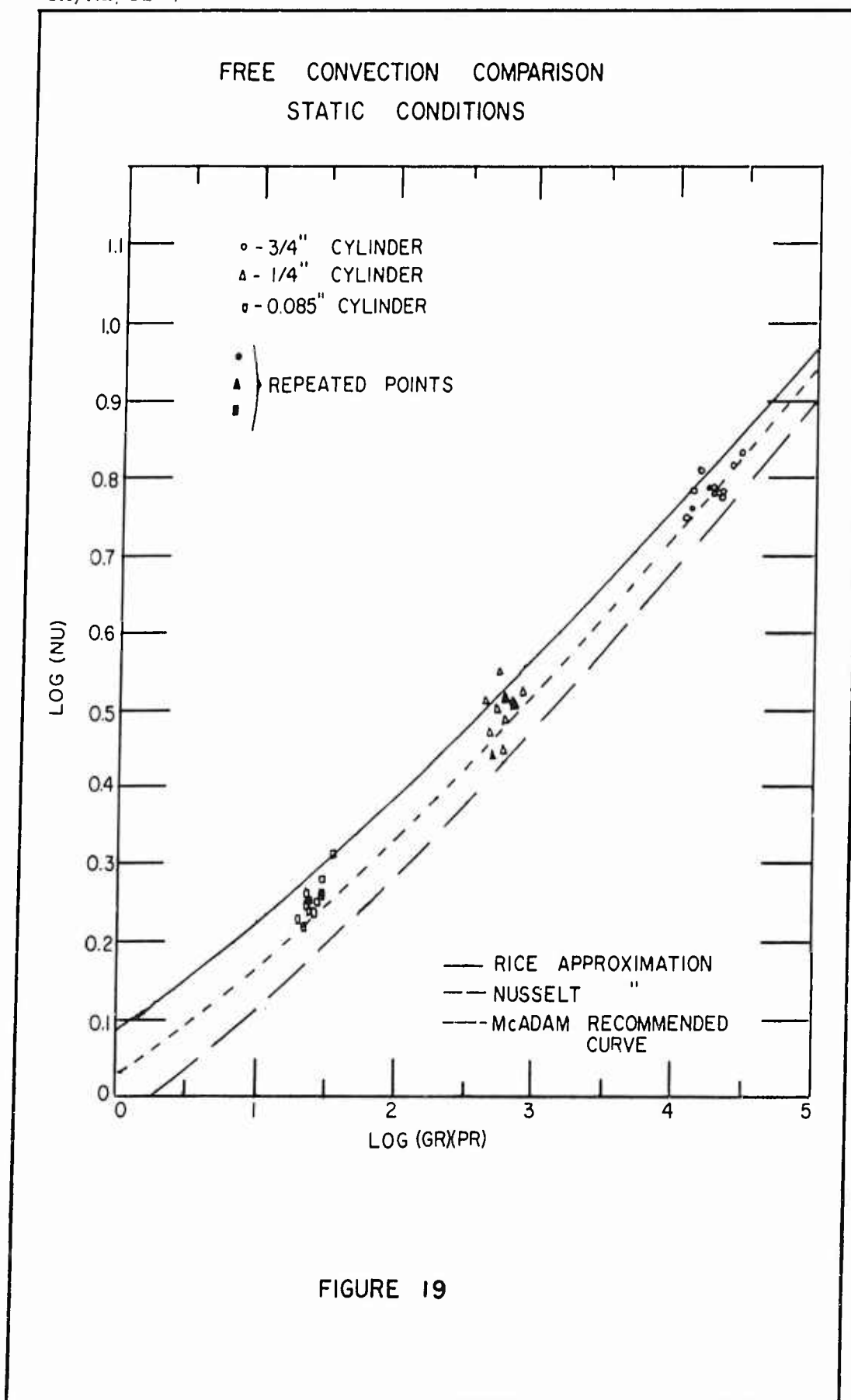
FIGURE 19

Analysis of Calculations

The heat loss through convection could be determined by two methods: first, by subtracting the radiation and the conduction losses from the power in the heater element, and second, by subtracting the line, meter, radiation, and conduction losses from the total power in the circuit. The second method was employed because of the difficulty in securing the lead wires of the voltmeter to the junction points of the heater element in the cylinder under high vibration intensities. However, the first method was employed statically to the 3/4 and 0.085 inch cylinder to check the heat loss by convection without having to account for the line and meter losses. The two methods at the static condition where within 7% of each other.

Conduction Losses

Conduction losses through the support rods where determined for the three cylinders by applying the equation:

$$Q_D = kA_c \Delta\theta/\Delta y \tag{11}$$

The thermal conductivities (k) were determined to be 0.134 BTU/ hr ft ^oF for the two phenolic supports on the 3/4 inch cylinder, and 16.7 BTU/hr ft ^oF for the stainless steel support rods (Ref 7:497). The quantities $\Delta\theta$ and Δy where determined by placing one thermocouple at the support rod-cylinder junction and another approximately 1/4 inch away from the cylinder on the support rod. Various temperature

47

differences (ΔT) between the cylinder surface and the ambient
environment were set, and the temperature difference ($\Delta\theta$)
recorded. A plot of the findings is shown in Figures 20 and
21. Knowing the temperature difference (ΔT), the above charts
can be entered to find $\Delta\theta$. The 0.085 inch cylinder was
vibrated to determine the effect of vibration on conduction
through the support rods. A static temperature increment (ΔT)
of 70°F was established, and increasing vibration intensities
were employed. At the various vibration intensity levels the
temperature increment $\Delta\theta$ was recorded. The results of this
study are shown in Figure 21. As the vibration intensity
increased, the value of $\Delta\theta$ decreased in the same manner as ΔT
decreased. From this it was concluded that the vibration
effects on conduction through the support rods corresponds
directly to the difference between the surface temperature and
ambient temperature. Therefore, in determining the conduction
loss of a vibrating cylinder only the surface and ambient
temperatures were required.

From the above study it was found that the conduction
loss through the two phenolic support rods on the 3/4 inch
cylinder was less than 1% of the total power. Therefore,
conduction losses were assumed to be negligible for this
cylinder. Since the thermal conductivity of phenolic is
relatively small the conduction losses of the two outside
supports on the 1/4 inch cylinder were also assumed to be
negligible. The two middle support rods of stainless steel
were found to cause a conduction loss as high as 18.5% of

48

CONDUCTION LOSS
DETERMINATION
FOR 0.25 IN. CYLINDER

FIGURE 20

$\Delta\theta - °F$

$\Delta T - °F$

CONDUCTION LOSS
DETERMINATION
FOR 0.085 IN. CYLINDER
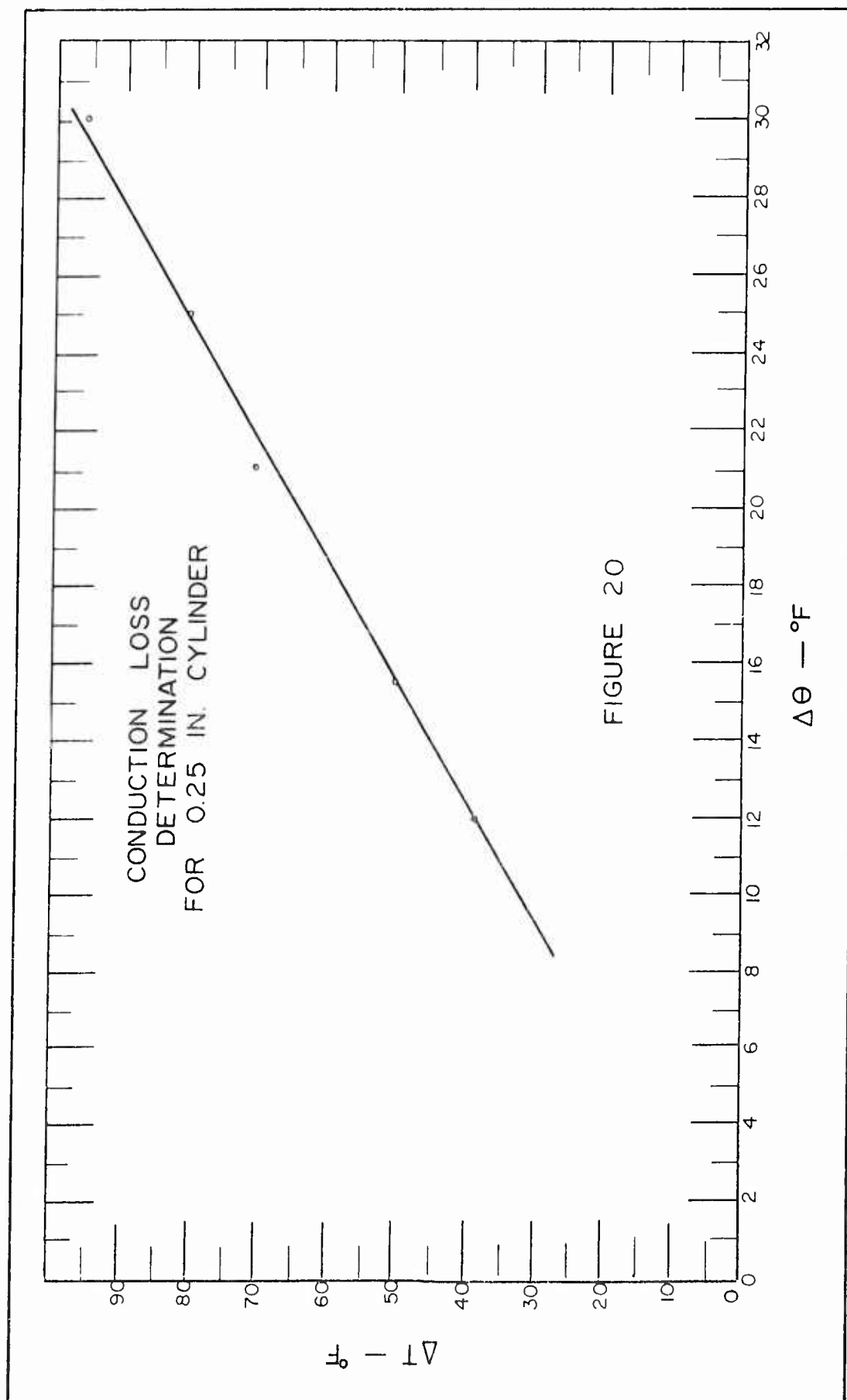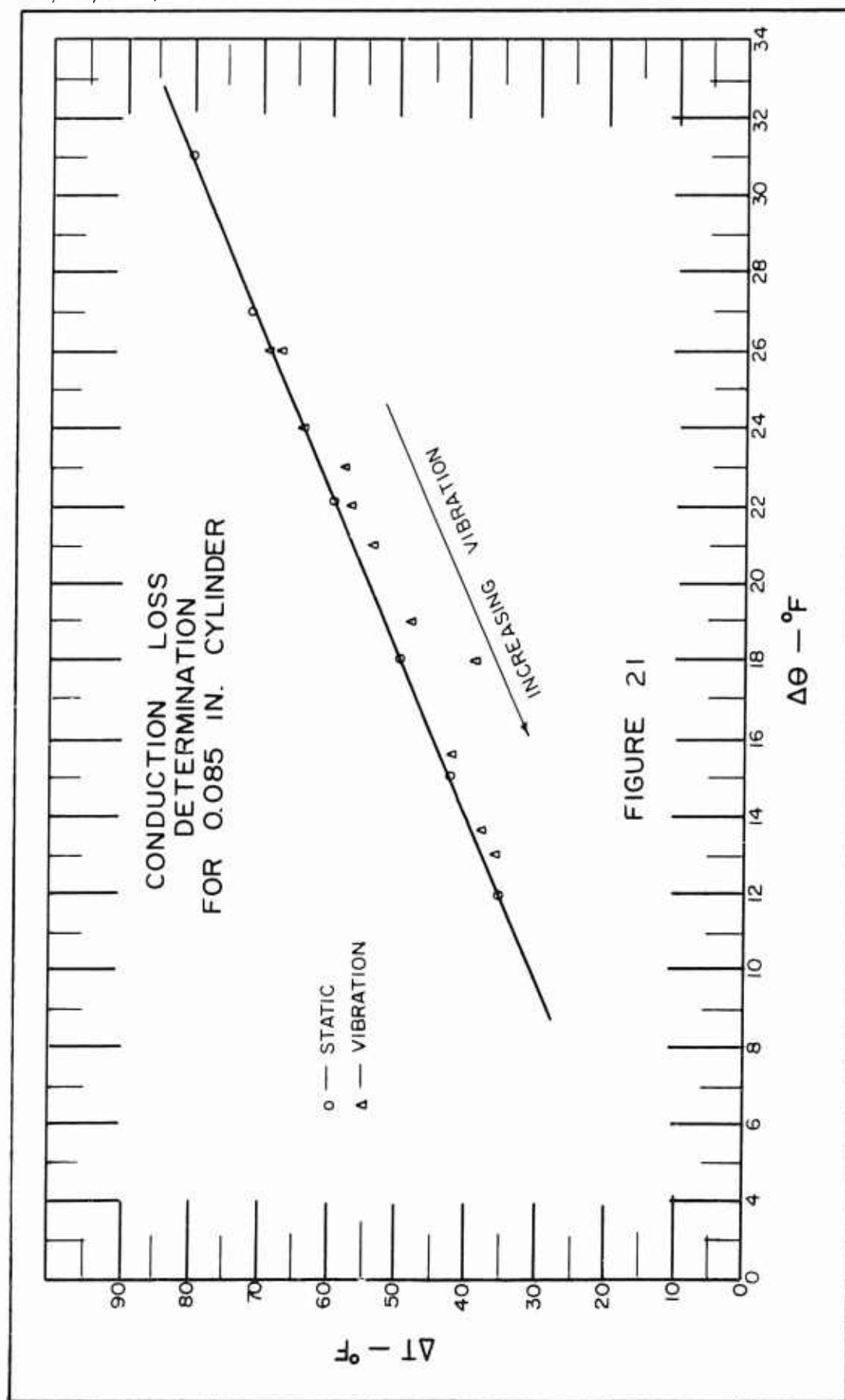
FIGURE 21

the total power at elevated surface temperatures. Conduction losses were computed for every data point in the investigation of the 1/4 inch cylinder. The conduction losses for the 0.085 inch cylinder were in the vicinity of 10% of the total power. This conduction loss was based on all four support rods.

The equations for the heat loss through conduction were simplified by substituting into equation (11) the appropriate values of the thermal conductivity of the support rods, the cross section area of the support rods, and the distance between the thermocouples on the support rods. The resulting equations are:

$$Q_D = 0.0334\Delta\theta \tag{3}$$

and

$$Q_D = 0.0128\Delta\theta \tag{4}$$

where $\Delta\theta$ is read directly from the appropriate curves of Figures 20 and 21.

Radiation Losses

Radiation losses were determined from the equation:

$$Q_R = 0.2931\sigma\epsilon A(T_{rw}^4 - T_{ra}^4) \tag{5}$$

The emissivity of the 3/4 and 1/4 inch cylinders was assumed to be 0.061 (Ref 8:151). For the 0.085 inch cylinder, the emissivity was assumed to be 0.21 (Ref 7:514).

Radiation power loss for the three cylinders was determined for various cylinder wall and ambient temperatures. These results are shown in Figures 22, 23, and 24. From these curves

51
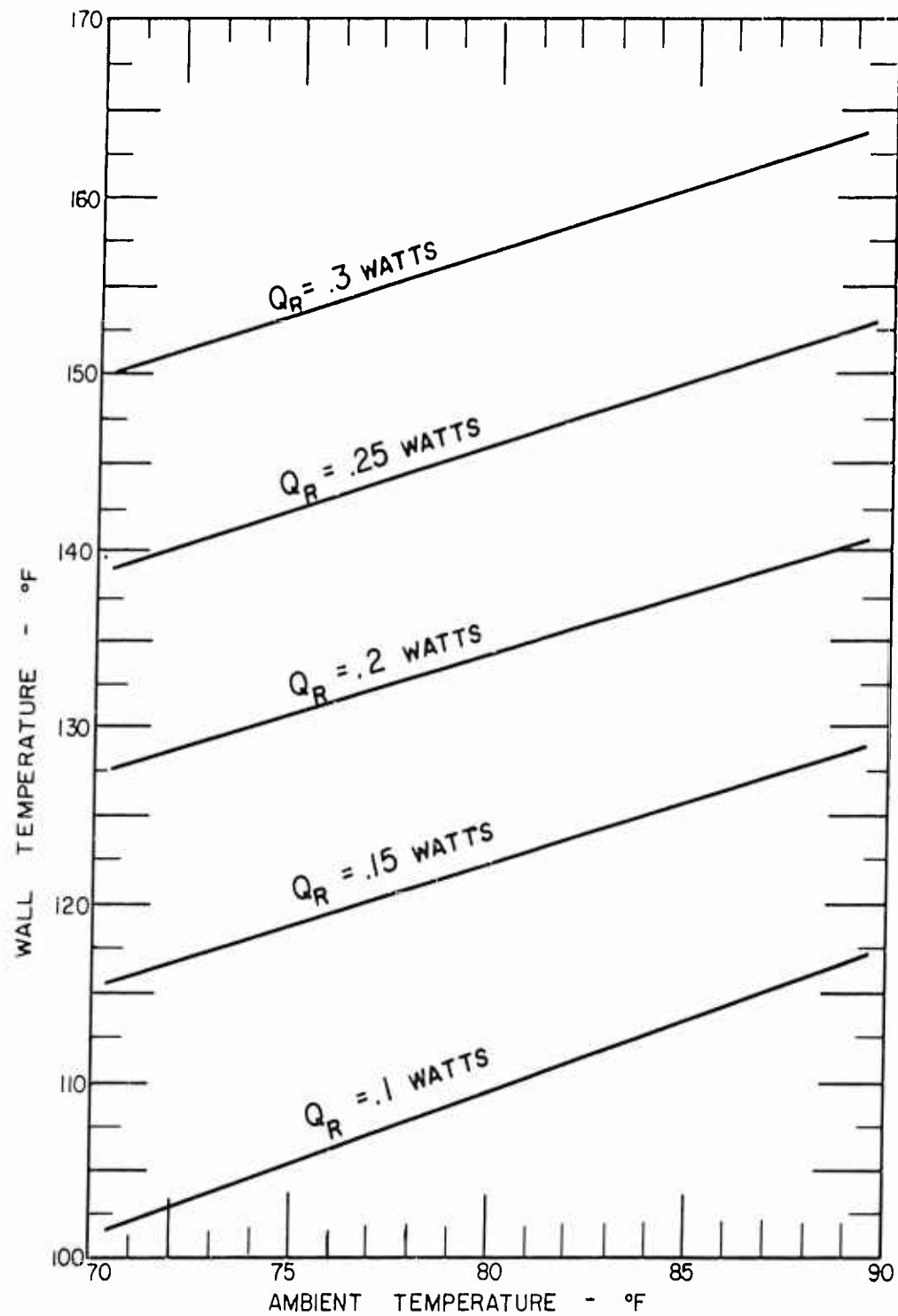
RADIATION   LOSS
FOR   3/4 IN. CYLINDER

FIGURE 22

RADIATION LOSS
FOR 1/4 IN. CYLINDER
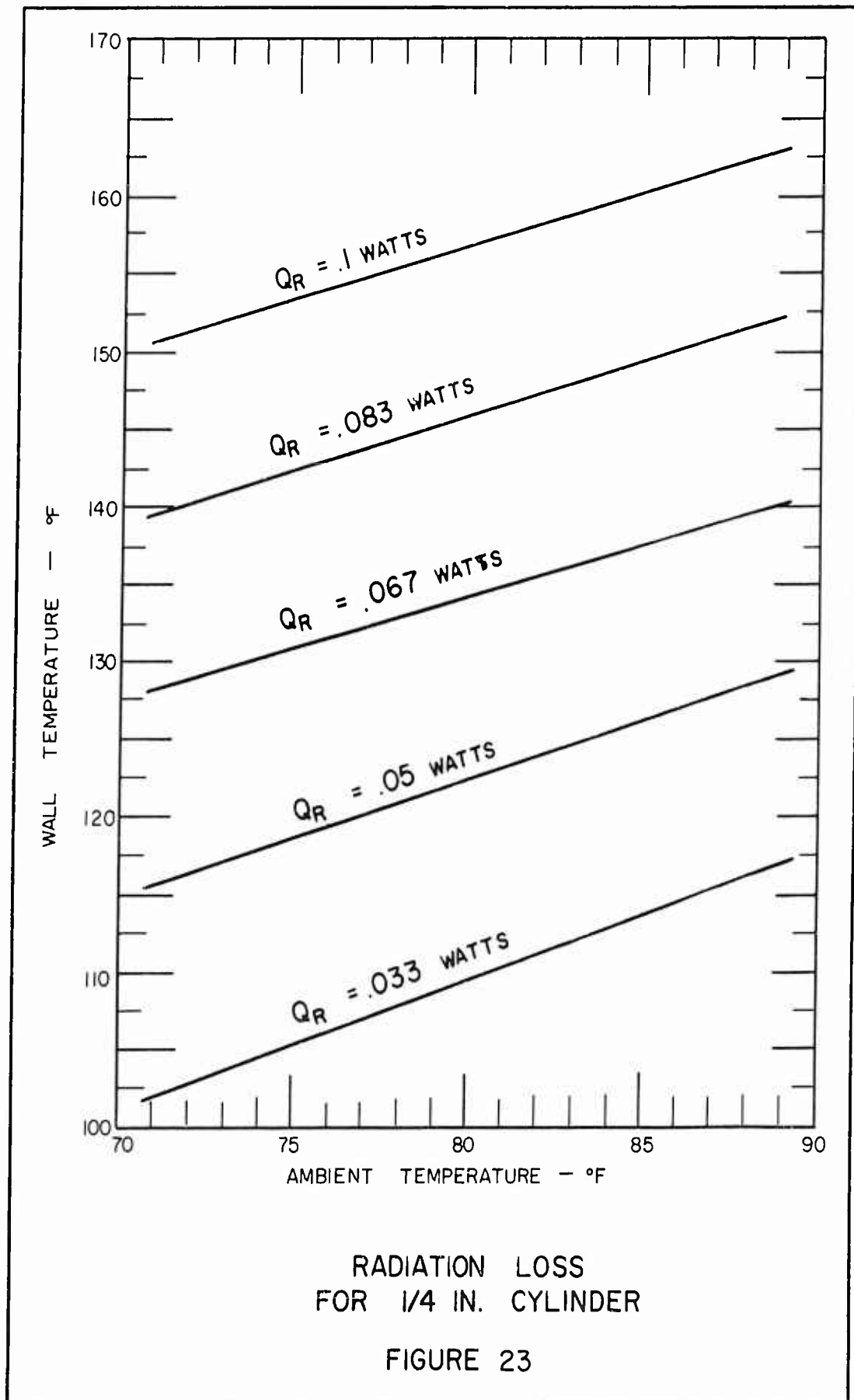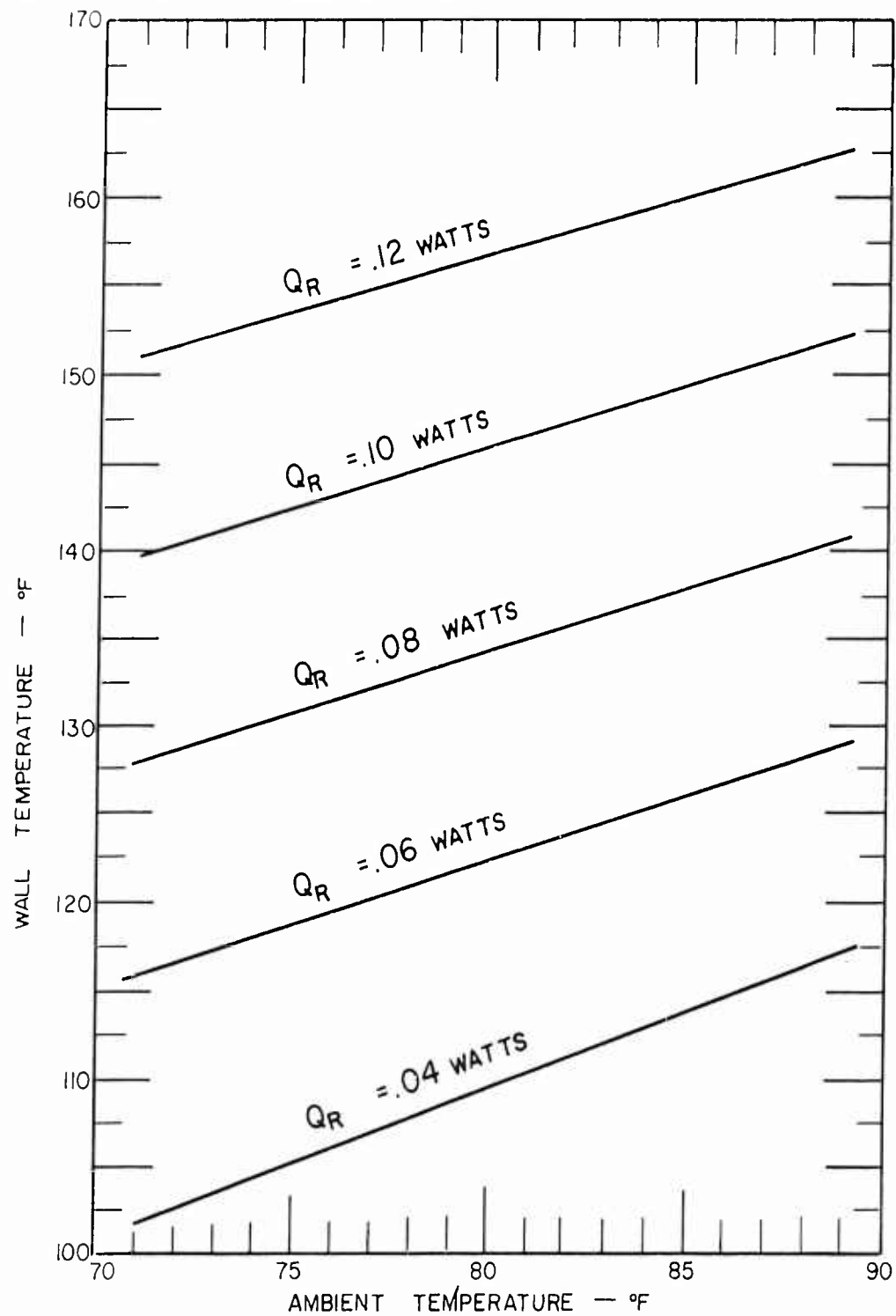
FIGURE 23

RADIATION LOSS
FOR 0.085 IN. CYLINDER

FIGURE 24

the radiation loss can be determined directly.

The maximum power loss due to radiation was found to be less than 4½% of the total power for the 3/4 inch cylinder. This loss was less than 2½% for the 1/4 inch cylinder, and less than 3% for the 0.085 inch cylinder.

Line Losses

Since the heater wires in the 3/4 and 1/4 inch cylinders were internally installed, the voltage was measured through the heater element and the lead wires. This involved determining the heat loss in the lead wires. This heat loss was determined from the equation:

$$Q_L = I^2 R \qquad (6)$$

The 3/4 and 0.085 inch cylinders employed the same type lead wires. The resistance of the wires was calculated to be 0.083 ohms for 13 feet of wire (Ref 9:202). At maximum temperature difference the power lost in the lines of the 3/4 inch cylinder was less than 1% of the total power. Therefore, the line loss in the cylinder was considered negligible. Due to the large current required in the 0.085 inch cylinder, the line loss was as high as 40% of the total power. This loss was considered at every data point.

The 1/4 inch cylinder employed a smaller lead wire in order to fit inside the ceramic insulator tube. The resistance for this cable was determined to be 0.123 ohms for 13 feet of wire (Ref 9:202). The maximum power dissipated in this lead

cable was found to be less than 4% of the total power. Line losses were also considered for this cylinder.

The resistance of the wires used above was based on standard conditions. Since the operation temperatures in this investigation exceeded the standard value for temperature by only 100 ^{O}F, the change in resistance produced only a 2% difference from the value used.

Meter Losses

Heat loss in the type meters employed was determined from the equation:

$$Q_M = I^2R \tag{6}$$

The resistance of the meters was measured with a Wheatstone Bridge. The resistance of the meter was 0.094 ohms for the 3/4 inch cylinder investigation, 0.047 ohms for the 1/4 inch cylinder investigation, and 0.02 ohms for the 0.085 inch cylinder investigation.

The heat loss in the meter of the 3/4 inch cylinder was found to be less than 1% of the total power. Meter losses were assumed negligible in this case. The meter loss in the 1/4 inch cylinder was found to be less than 2% of the total power. The meter loss in the 0.085 inch cylinder was found to be as high as 9% of the total power.

End Losses

The end losses were considered to be negligible in this investigation for all cylinders. This assumption was based

on the comparison of the lateral surface area to the end

surface area. In all cases the effective end area was found

to be less than 5% of the lateral surface area. Also, the

two large cylinders employed end caps of low thermal conductivity.

APPENDIX C

Mechanical Drawings of Cylinder

Assemblies and Dimensions

TOP VIEW

NO.	NOMENCLATURE
①	LIGHT SOURCE
②	LIGHT FILTER
③	SMALL MIRROR
④	PARABOLIC MIRROR
⑤	BEAM SPLITTER
⑥	INTERFEROMETER
⑦	MIRROR
⑧	VIBRATOR
⑨	RESONATOR
⑩	CYLINDER
⑪	LENS
⑫	CAMERA

FIG. NO.
25

SCHEMATIC DIAGRAM
OF APPARATUS
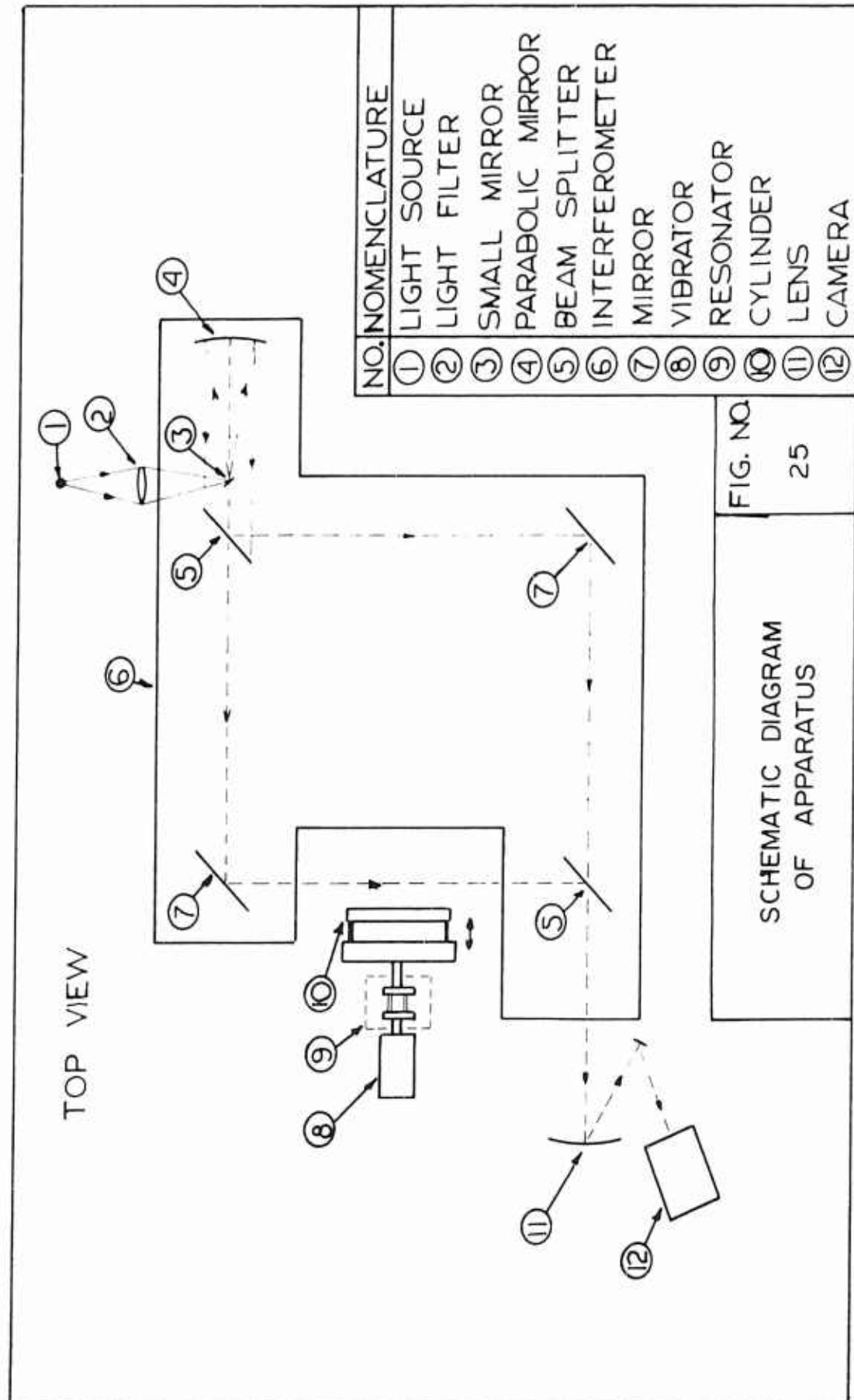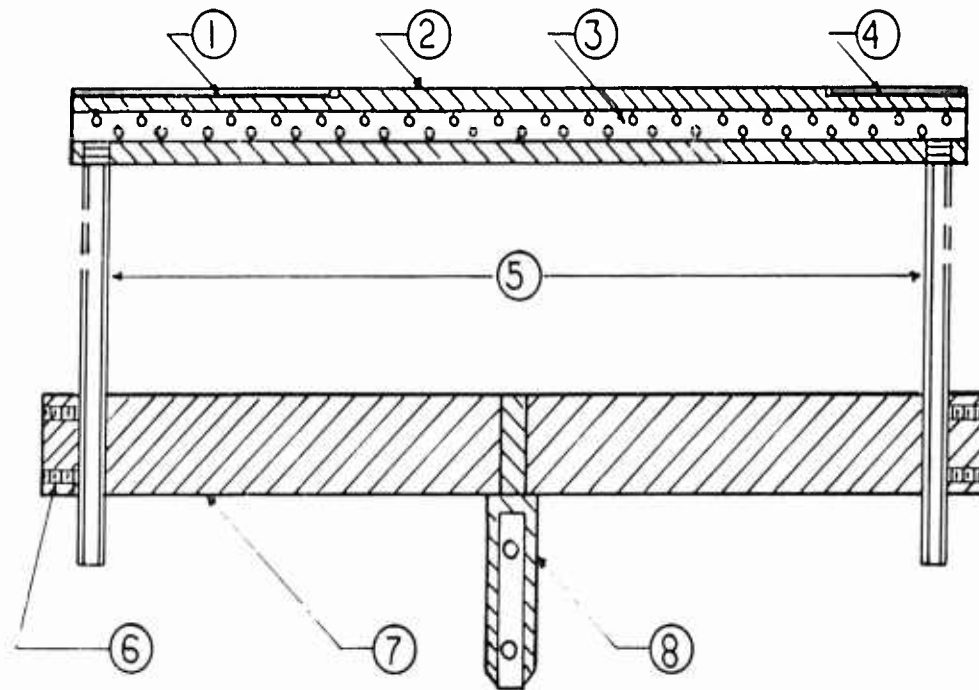
NO.	NOMENCLATURE	NO. REQ.	MATERIAL
①	THERMOCOUPLE NO 1	1	IRON CONST.
②	TEST CYLINDER	1	24 ST ALUMINUM
③	HEATER	1	NICHROME
④	THERMOCOUPLE NO 2	1	IRON CONST
⑤	SUPPORT RODS	2	PHENOLIC
⑥	ALLEN SCREWS	4	STEEL
⑦	MAIN SUPPORT ROD	1	ALUMINUM
⑧	MOUNT BRACE	1	STEEL

NO. REQ.	SCALE	MATERIAL	DRAWN BY	
1	1/2" = 1"	AS SHOWN	RMR	

TITLE	FIG. NO.
3/4" CYLINDER ASSEMBLY	26

3/4" TEST CYLINDER

NO.	NAME	NO. REQ	MATERIAL		DRAWN BY	SCALE
					RMR	1/2" = 1"
1	TEST CYLINDER	1	24-ST ALUM.			
2	SUPPORT RODS	2	PHENOLIC		TITLE	
3	MAIN SUPPORT RODS	1	24-ST ALUM.		3/4" TEST CYLINDER	
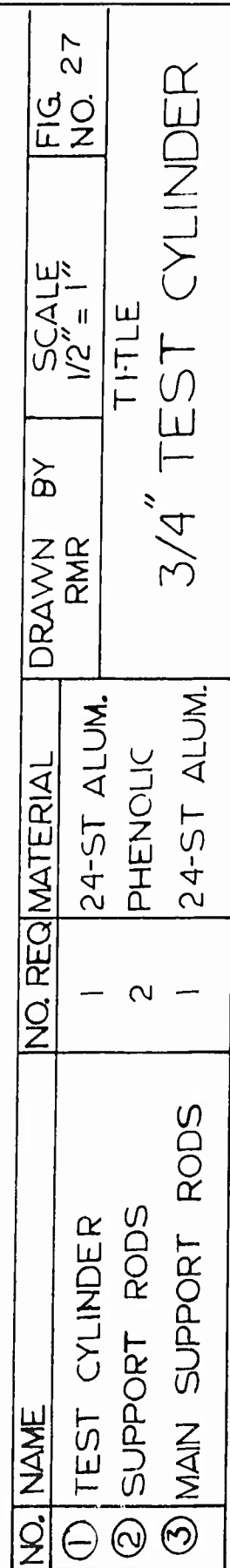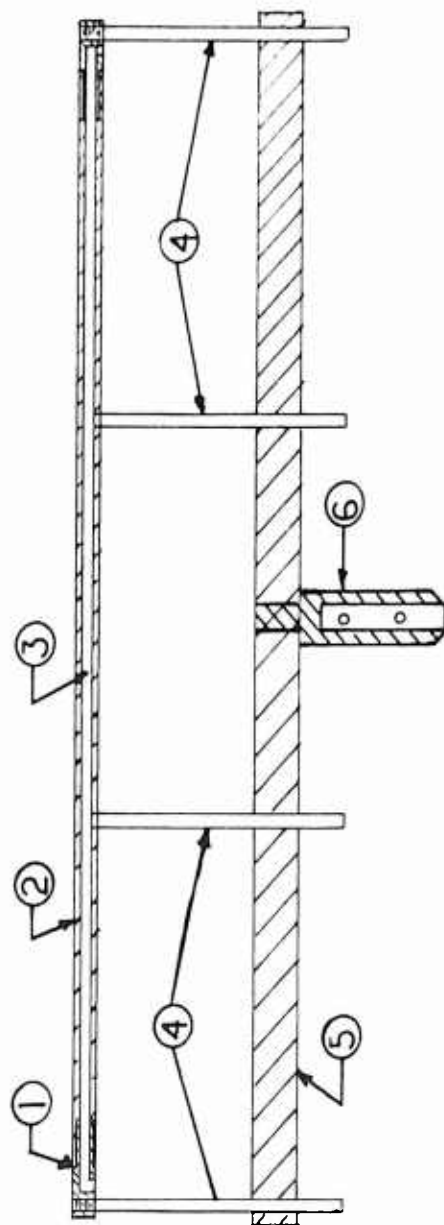
FIG. NO. 27

NOMENCLATURE	NO REQ	MATERIAL
① END CAPS	2	PHENOLIC
② TEST CYLINDER	1	24 ST ALUM
③ HEATER	1	NICHROME
④ SUPPORT RODS	4	STEEL
⑤ MAIN SUPPORT ROD	1	ALUM STOCK
⑥ MOUNT BRACE	1	STEEL

DRAWN BY	SCALE	FIG
RMR	1/2" = 1"	NO 28

TITLE

1/4" CYLINDER ASSEMBLY

1/4" TEST CYLINDER

NO	NAME	NO REQ	MATERIAL
1	TEST CYLINDER	1	24 ST ALUM
2	END CAPS	2	PHENOLIC
3	SUPPORT RODS	4	STEEL
4	MAIN SUPPORT ROD	1	ALUM. STOCK

DRAWN BY RMR

SCALE 1/2" = 1"

FIG. NO. 29

TITLE
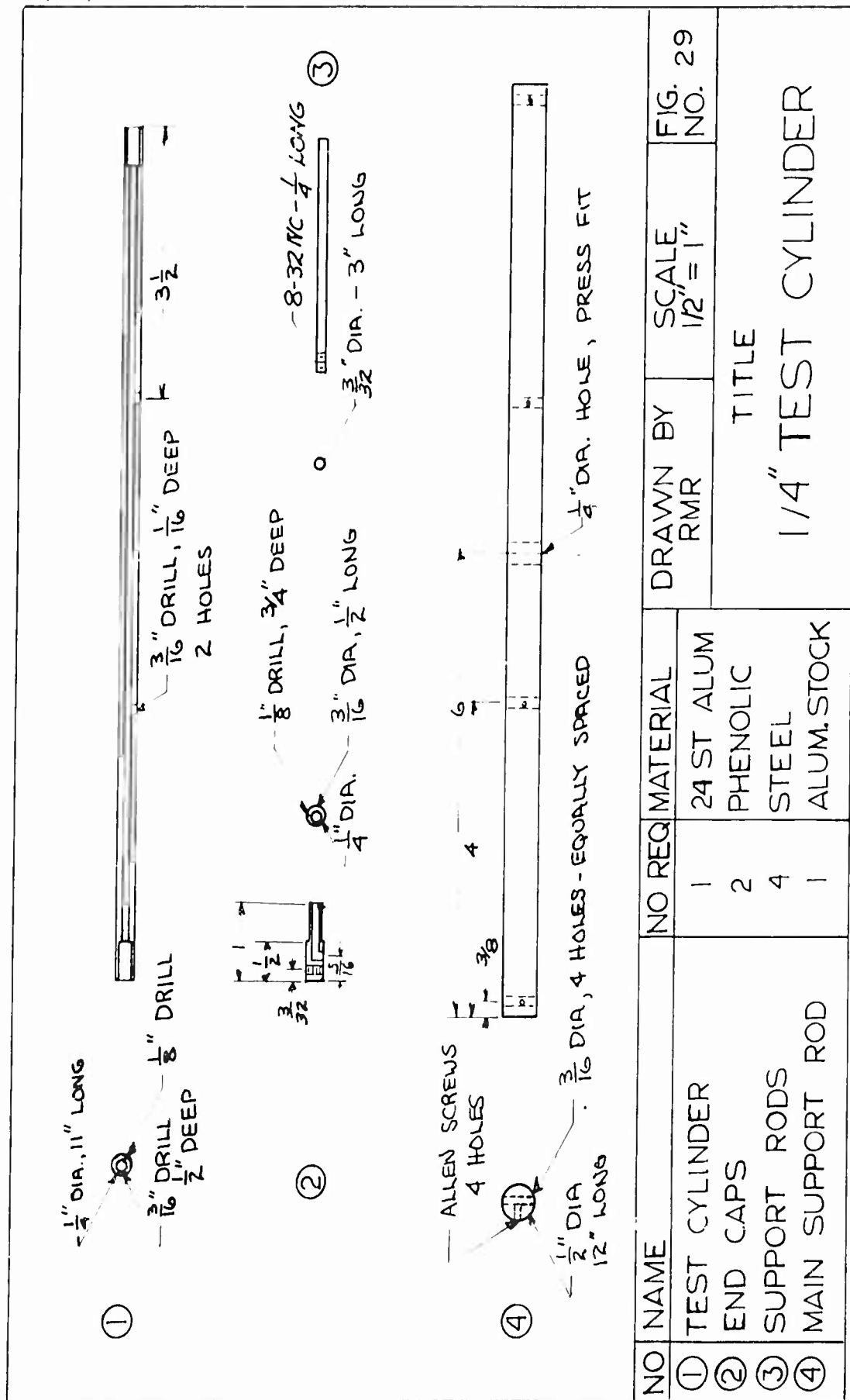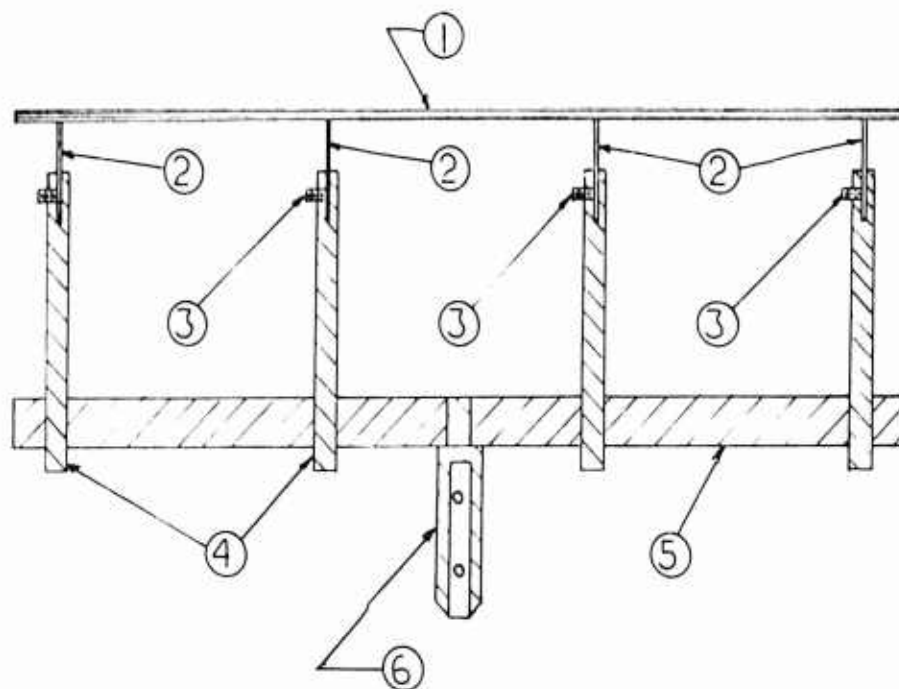
NO.	NOMENCLATURE	NO. REQ.	MATERIAL
①	TEST CYLINDER	1	STEEL
②	FIXED SUPPORTS	4	STEEL
③	ALLEN SCREWS	4	STEEL
④	SUPPORT RODS	4	PHENOLIC
⑤	MAIN SUPPORT ROD	1	ALUM. STOCK
⑥	MOUNT BRACE	1	STEEL

NO. REQ. 1	SCALE 1/2"= 1"	MATERIAL AS SHOWN	DRAWN BY RMR	
TITLE				FIG. NO.
0.085" CYLINDER ASSEMBLY				30

0.0085" TEST CYLINDER

FIG. 31
NO.

NO.	NAME	NO.REQ.	MATERIAL
①	TEST CYLINDER	1	STEEL
②	SUPPORT RODS	1	PHENOLIC
③	MAIN SUPPORT ROD	1	ALUM.

DRAWN BY
RMR

SCALE
1/2"= 1"

TITLE
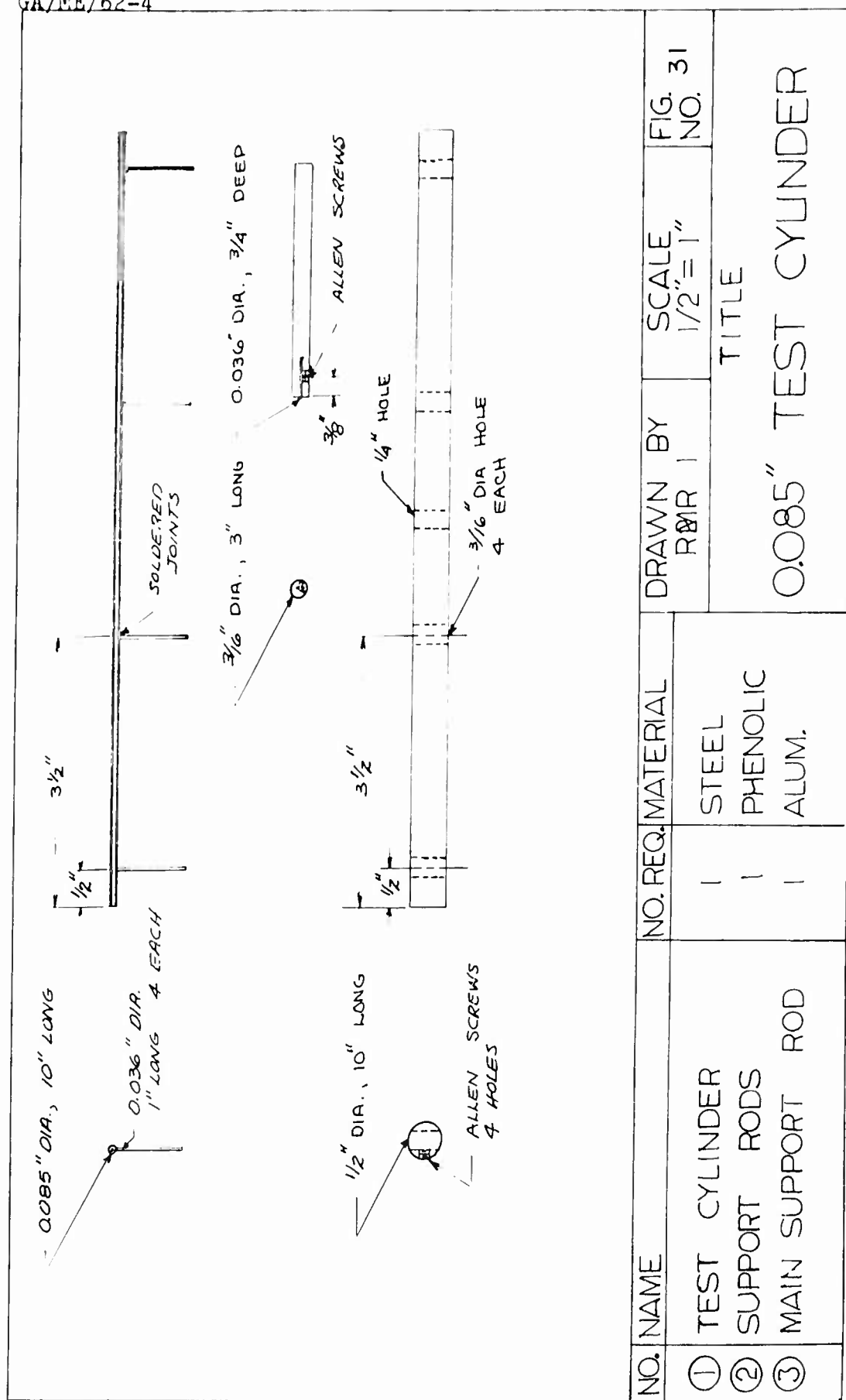
APPENDIX D

Sample Calculation

Sample Calculation

The following calculation is based on run #16 of the
1/4 inch cylinder investigation. The recorded values were:

$$T_w = 133.7 \ ^oF$$
$$T_a = 89 \ ^oF$$
$$E = 4.35 \ \text{volts}$$
$$I = 1.17 \ \text{amps}$$
$$H = 0.2066 \ \text{inches}$$
$$f = 85 \ \text{cps}$$

From this data the effect of vibration on the heat transfer
rate was computed from the equations:

$$Q_T = EI = (4.35)(1.17) = 5.08 \ \text{watts}$$

$$Q_L = I^2R = (1.17)^2(0.123) = 0.17 \ \text{watts}$$

$$Q_M = I^2R = (1.17)^2(0.047) = 0.06 \ \text{watts}$$

$$Q_R = 0.2931 \sigma \epsilon A(T_{rw}^{4} - T_{ra}^{4}) = 0.05 \ \text{watts}$$

where the value for Q_R was read from Figure 24 of Appendix B
for a T_w of 133.7 ^oF and T_a of 89 ^oF.

$$Q_D = 0.0334 \Delta\theta = 0.0334(13.7) = 0.46 \ \text{watts}$$

where $\Delta\theta$ was read from Figure 21 of Appendix B for a ΔT of
44.7 ^oF.

$$Q_C = Q_T - Q_L - Q_M - Q_R - Q_D = 4.34 \ \text{watts}$$

$$Nu = 1.3 \ Q_C/k_f \Delta T = 1.3(4.34)/(0.01595)(44.7) = 7.91$$

where 1.3 is the conversion factor with the dimensions of
BTU/watt hr ft. The value of k_f was determined from tables

67

GA/ME/62-4

of Eckert and Drake (Ref 7:504).

$$Nu/Pr^{.3} = (7.91)/(0.704)^{.3} = 8.80$$

where the Pr was determined from tables of Eckert and Drake (Ref 7:504).

$$Re_v = 4afd/144\nu_f = (0.413)(85)(0.25)/144(18.85)10^{-5}$$
$$= 322$$

where 4a is the total distance traveled during one cycle and is equivalent to 2H. The 144 is the conversion factor of in^2 to ft^2. The value of ν_f was determined from tables of Eckert and Drake (Ref 7:504).

APPENDIX E

Experimental Data

Table I

General Data 1/4 in. Diameter Cylinder

Run	T_w °F	T_a °F	Q_T watts	Freq cyc/sec.	Total Disp. 2H in.	ΔT °F	Q_L watts	Q_M watts	Q_R watts	Q_D watts	Q_C watts	Nu	Re_v
1	167.0	77.0	5.03	0	0	90.0	0.17	0.06	0.12	0.91	3.77	3.36	0
2	140.3	77.3	5.03	115	0.236	63.0	0.17	0.06	0.08	0.65	4.07	5.29	251
3	146.8	77.3	5.03	115	0.191	69.5	0.17	0.06	0.09	0.70	4.01	4.70	201
4	150.3	77.3	5.03	115	0.183	73.0	0.17	0.06	0.10	0.74	3.94	4.38	192
5	154.1	77.3	5.03	115	0.158	76.8	0.17	0.06	0.10	0.77	3.91	4.12	164
6	159.0	77.0	5.03	115	0.133	82.0	0.17	0.06	0.11	0.83	3.84	3.78	137
7	161.7	76.7	5.03	115	0.106	85.0	0.17	0.06	0.11	0.86	3.81	3.61	109
8	164.2	76.7	5.03	115	0.096	87.5	0.17	0.06	0.12	0.89	3.77	3.47	98
9	166.3	76.6	5.03	115	0.078	89.7	0.17	0.06	0.12	0.91	3.75	3.35	80
10	167.3	76.6	5.13	115	0.068	90.7	0.17	0.06	0.12	0.91	3.85	3.40	70
11	167.3	76.5	5.13	115	0.030	90.8	0.17	0.06	0.12	0.91	3.86	3.40	30
12	132.5	76.5	5.13	115	0.262	56.0	0.17	0.06	0.08	0.57	4.25	6.25	283
13	117.3	89.3	5.08	84	0.602	28.0	0.17	0.06	0.03	0.28	4.54	13.40	475
14	122.7	89.2	5.08	84	0.498	33.5	0.17	0.06	0.04	0.35	4.46	10.95	389
15	125.7	89.1	5.08	84	0.463	36.6	0.17	0.06	0.04	0.38	4.43	9.93	360
16	133.7	89.0	5.08	85	0.413	44.7	0.17	0.06	0.05	0.46	4.34	7.91	322
17	144.0	89.0	5.08	86	0.330	55.0	0.17	0.06	0.07	0.56	4.22	6.21	256
18	151.7	84.0	3.67	0	0	67.7	0.12	0.05	0.09	0.69	2.72	3.24	0
19	128.5	84.5	3.67	115	0.280	44.0	0.12	0.05	0.05	0.43	3.02	5.64	302
20	134.5	84.5	3.74	115	0.235	50.0	0.12	0.05	0.06	0.51	3.00	4.90	249
21	143.0	85.0	3.74	115	0.165	58.0	0.13	0.05	0.07	0.59	2.91	4.07	173
22	144.8	85.3	3.80	115	0.140	59.5	0.13	0.05	0.07	0.61	2.95	4.00	146
23	146.3	85.3	3.80	115	0.127	61.0	0.13	0.05	0.08	0.62	2.93	3.89	129
24	150.0	85.5	3.80	115	0.090	64.5	0.13	0.05	0.08	0.65	2.90	3.63	93
25	152.0	85.5	3.80	115	0.075	66.5	0.13	0.05	0.08	0.68	2.87	3.48	79
26	153.0	85.5	3.80	115	0.048	67.5	0.13	0.05	0.09	0.69	2.86	3.40	49
27	155.0	85.5	3.80	115	0.028	69.5	0.13	0.05	0.09	0.71	2.84	3.28	29
28	149.0	79.0	3.62	115	0.025	70.0	0.12	0.05	0.09	0.71	2.75	3.19	25
29	124.0	79.0	3.62	115	0.244	45.0	0.12	0.05	0.06	0.46	2.92	5.33	267
30	113.7	91.0	3.67	84	0.530	22.7	0.12	0.05	0.02	0.25	3.23	11.85	422

Table I (cont.)

Run	T_w °F	T_a °F	Q_T watts	Freq cyc/sec	Total Disp. in.	ΔT °F	Q_L watts	Q_M watts	Q_R watts	Q_D watts	Q_C watts	Nu	Re_v
31	116.0	91.0	3.67	84	0.475	25.0	0.12	0.05	0.02	0.27	3.21	10.65	375
32	117.3	91.0	3.67	84	0.433	26.3	0.12	0.05	0.03	0.29	3.18	10.00	341
33	122.3	91.0	3.67	85	0.412	31.3	0.12	0.05	0.04	0.33	3.13	8.14	327
34	128.7	91.0	3.67	86	0.358	37.7	0.12	0.05	0.05	0.38	3.07	6.51	284
35	127.5	80.5	2.32	0	0	47.0	0.08	0.03	0.06	0.48	1.67	2.93	0
36	112.5	80.5	2.32	115	0.251	32.0	0.08	0.03	0.03	0.32	1.86	4.85	280
37	115.5	80.5	2.32	115	0.184	35.0	0.08	0.03	0.04	0.35	1.82	4.33	202
38	121.5	80.5	2.32	115	0.126	41.0	0.08	0.03	0.05	0.42	1.74	3.53	137
39	125.5	80.5	2.32	115	0.065	45.0	0.08	0.03	0.05	0.46	1.70	3.12	71
40	127.5	80.5	2.32	115	0.038	47.0	0.08	0.03	0.06	0.48	1.67	2.93	41
41	117.0	78.0	2.32	115	0.145	39.0	0.08	0.03	0.05	0.40	1.76	3.76	160
42	120.0	78.0	2.32	115	0.104	42.0	0.08	0.03	0.05	0.43	1.73	3.42	113
43	124.7	79.2	2.25	115	0.030	45.5	0.08	0.03	0.06	0.48	1.60	2.91	32
44	103.0	88.0	2.36	84	0.567	15.0	0.08	0.03	0.01	0.17	2.07	11.50	458
45	107.7	88.0	2.36	84	0.439	19.7	0.08	0.03	0.01	0.18	2.06	8.70	352
46	105.3	87.8	2.36	84	0.480	17.5	0.08	0.03	0.01	0.17	2.07	10.90	386
47	110.3	87.8	2.36	85	0.398	22.5	0.08	0.03	0.03	0.21	2.01	7.40	322
48	117.0	87.8	2.36	85	0.347	29.2	0.08	0.03	0.03	0.30	1.92	5.45	279

71

Table II

General Data 0.085 in. Diameter Cylinder

Run	T_w °F	T_a °F	Q_T watts	Freq cyc/sec	Total Disp. 2Hp in.	ΔT °F	Q_L watts	Q_M watts	Q_R watts	Q_D watts	Q_C watts	Nu	Re_v
1	164.7	82.7	4.41	0	0	82.0	1.58	0.38	0.13	0.41	1.91	1.86	0
2	131.3	82.8	4.41	115	0.2716	48.5	1.58	0.38	0.08	0.24	2.13	3.36	98.5
3	141.0	83.0	4.41	115	0.2288	58.0	1.58	0.38	0.09	0.27	2.09	2.93	82.4
4	149.0	83.2	4.41	115	0.1948	65.8	1.58	0.38	0.10	0.32	2.03	2.50	68.8
5	155.8	83.3	4.41	115	0.1718	72.5	1.58	0.38	0.11	0.34	2.00	2.23	60.0
6	158.8	83.3	4.41	115	0.1246	75.5	1.58	0.38	0.11	0.37	1.97	2.09	43.6
7	161.0	83.4	4.41	115	0.1044	77.6	1.58	0.38	0.12	0.39	1.94	1.99	36.2
8	162.5	83.5	4.41	115	0.0736	79.0	1.58	0.38	0.13	0.40	1.92	1.96	25.4
9	163.7	83.5	4.41	115	0.0560	80.2	1.58	0.38	0.13	0.40	1.91	1.90	19.4
10	110.0	85.0	4.33	84	0.6532	25.0	1.50	0.36	0.04	0.10	2.33	7.79	180.0
11	111.0	85.0	4.33	84	0.6104	26.0	1.50	0.36	0.04	0.10	2.33	7.49	164.5
12	113.0	85.0	4.33	84.0	0.5470	28.0	1.50	0.36	0.04	0.11	2.32	6.90	144.0
13	117.0	85.0	4.33	84	0.4726	32.0	1.50	0.36	0.04	0.13	2.32	5.95	128.5
14	125.3	85.0	4.33	84	0.3656	40.3	1.50	0.36	0.06	0.18	2.23	4.56	97.8
15	138.3	85.0	4.33	84	0.3000	53.3	1.50	0.36	0.08	0.25	2.14	3.26	78.5
16	147.7	85.0	4.33	84	0.2746	62.5	1.50	0.36	0.10	0.30	2.07	2.69	70.8
17	159.7	85.0	4.33	84	0.2178	74.2	1.50	0.36	0.12	0.36	1.99	2.15	55.2
18	141.0	79.4	3.22	0	0	61.6	1.15	0.27	0.12	0.30	1.41	1.83	0
19	118.3	79.5	3.22	115	0.2774	38.8	1.15	0.27	0.09	0.17	1.58	3.39	94.0
20	122.7	79.7	3.22	115	0.2336	43.0	1.15	0.27	0.06	0.19	1.55	3.31	86.5
21	126.0	80.0	3.22	115	0.2006	46.0	1.15	0.27	0.07	0.21	1.52	2.72	74.0
22	130.7	80.4	3.22	115	0.1804	50.3	1.15	0.27	0.07	0.23	1.50	2.45	66.0
23	136.0	80.5	3.22	115	0.1480	55.5	1.15	0.27	0.08	0.26	1.46	2.16	53.6
24	137.7	80.5	3.22	115	0.1312	57.2	1.15	0.27	0.09	0.27	1.44	2.06	47.6
25	139.0	80.5	3.22	115	0.0860	58.5	1.15	0.27	0.09	0.28	1.43	2.00	31.2
26	141.3	80.5	3.22	115	0.0666	60.8	1.15	0.27	0.09	0.30	1.41	1.83	24.2
27	103.7	84.8	3.22	84	0.6650	18.9	1.14	0.27	0.02	0.07	1.71	7.60	181.0
28	105.7	84.9	3.22	84	0.5664	20.8	1.14	0.27	0.03	0.08	1.69	6.79	156.5
29	107.3	84.9	3.22	84	0.5460	22.4	1.14	0.27	0.03	0.08	1.69	6.30	150.5
30	110.7	84.9	3.22	84	0.4520	25.8	1.14	0.27	0.04	0.10	1.66	5.36	124.5

Table II (cont.)

Run	T_w °F	T_a °F	Q_T watts	Freq cyc/sec	Total Disp. 2H in.	ΔT °F	Q_L watts	Q_M watts	Q_R watts	Q_D watts	Q_C watts	Nu	Re_v
31	112.0	85.0	3.22	84	0.4297	27.0	1.14	0.27	0.04	0.11	1.65	5.08	117.5
32	115.7	85.0	3.22	84	0.3790	30.7	1.14	0.27	0.05	0.13	1.63	4.40	103.0
33	118.0	85.0	3.22	84	0.3374	33.0	1.14	0.27	0.05	0.14	1.61	4.04	91.3
34	146.3	82.8	3.25	121	0.0284	63.5	1.14	0.27	0.10	0.31	1.43	1.83	10.7
35	145.7	83.0	3.25	121	0.1010	62.7	1.14	0.27	0.10	0.30	1.44	1.84	38.0
36	144.3	83.0	3.25	121	0.1326	61.3	1.14	0.27	0.09	0.29	1.45	1.93	49.8
37	141.7	82.7	3.25	121	0.1496	59.0	1.14	0.27	0.09	0.28	1.47	2.00	56.4
38	140.3	82.4	3.27	121	0.1772	57.9	1.14	0.27	0.09	0.28	1.47	2.08	66.8
39	134.3	82.3	3.27	121	0.2084	52.0	1.14	0.27	0.08	0.24	1.52	2.40	79.6
40	129.7	82.3	3.27	121	0.2188	47.4	1.14	0.27	0.07	0.22	1.55	2.71	84.4
41	123.3	82.3	3.30	121	0.2238	41.0	1.14	0.27	0.06	0.18	1.61	3.25	90.8
42	120.7	82.2	3.30	121	0.2418	38.4	1.14	0.27	0.05	0.17	1.63	3.92	99.2
43	132.7	82.3	2.37	0	0	49.0	0.88	0.21	0.07	0.22	0.99	1.66	0
44	113.7	83.7	2.37	115	0.2402	30.0	0.88	0.21	0.04	0.13	1.10	3.05	90.0
45	118.0	83.7	2.37	115	0.2162	34.0	0.88	0.21	0.05	0.15	1.07	2.61	80.8
46	120.1	84.1	2.37	115	0.1918	36.0	0.88	0.21	0.05	0.16	1.06	2.44	70.0
47	124.1	84.1	2.37	115	0.1774	40.0	0.88	0.21	0.06	0.18	1.03	2.12	65.0
48	126.2	84.2	2.37	115	0.1556	42.0	0.88	0.21	0.06	0.19	1.02	2.00	57.0
49	129.8	84.3	2.37	115	0.1298	45.5	0.88	0.21	0.07	0.21	1.00	1.80	47.4
50	131.0	84.4	2.37	115	0.0924	46.6	0.88	0.21	0.07	0.22	0.99	1.74	33.2
51	133.5	84.5	2.37	115	0.0584	49.0	0.88	0.21	0.07	0.22	0.99	1.66	21.2
52	98.3	83.5	2.38	84	0.6164	14.8	0.84	0.20	0.02	0.04	1.28	7.30	173.0
53	98.7	83.5	2.38	84	0.5796	15.2	0.84	0.20	0.02	0.04	1.28	7.10	163.0
54	99.3	83.5	2.38	84	0.5598	15.8	0.84	0.20	0.02	0.04	1.28	6.84	157.0
55	99.7	83.5	2.38	84	0.5450	16.2	0.84	0.20	0.02	0.04	1.28	6.66	153.0
56	104.0	83.5	2.38	84	0.4180	20.5	0.84	0.20	0.03	0.07	1.24	5.08	116.4
57	107.0	83.5	2.38	84	0.3600	23.5	0.84	0.20	0.04	0.09	1.21	4.29	99.0
58	110.0	83.5	2.38	84	0.3042	26.5	0.84	0.20	0.04	0.11	1.19	3.76	84.3
59	115.7	83.5	2.38	84	0.2778	31.2	0.84	0.20	0.04	0.13	1.17	3.12	76.0
60	128.0	83.5	2.38	84	0.1988	44.5	0.84	0.20	0.06	0.20	1.08	2.00	53.5
61	102.3	83.5	2.38	84	0.4612	18.8	0.84	0.20	0.02	0.06	1.26	5.64	129.0

Table III
General Data 3/4 in. Diameter Cylinder

Run	T_w °F	T_a °F	Q_T watts	Freq cyc/sec	Total Disp. 2H in.	ΔT °F	Q_L watts	Q_M watts	Q_R watts	Q_D watts	Q_C watts	Nu	Re$_v$
1	138.5	75.0	4.70	0	0	63.5	0.02	0.02	0.23	—	4.45	5.78	0
2	137.2	74.9	4.70	130	0.0760	62.3	0.02	0.02	0.21	—	4.47	5.90	278
3	130.0	75.0	4.70	130	0.1784	55.0	0.02	0.02	0.20	—	4.48	6.73	660
4	126.8	75.1	4.70	130	0.2240	51.7	0.02	0.02	0.18	—	4.50	7.23	828
5	133.5	75.1	4.70	130	0.1488	58.4	0.02	0.02	0.21	—	4.47	6.32	544
6	132.2	74.8	4.60	130	0.1068	57.4	0.02	0.02	0.20	—	4.38	6.25	391
7	133.5	74.8	4.60	130	0.1008	58.7	0.02	0.02	0.21	—	4.37	6.15	389
8	138.0	78.0	4.72	0	0	60.0	0.02	0.02	0.23	—	4.50	6.15	0
9	140.5	78.0	4.68	130	0.0556	62.5	0.02	0.02	0.23	—	4.43	5.76	214
10	141.5	78.0	4.65	130	0.1084	63.5	0.02	0.02	0.22	—	4.41	5.78	388
11	135.0	72.0	4.70	0	0	63.0	0.02	0.02	0.23	—	4.46	5.86	0
12	132.0	72.5	4.70	112	0.0896	59.5	0.02	0.02	0.21	—	4.47	6.25	284
13	130.1	73.1	4.70	112	0.1240	57.0	0.02	0.02	0.20	—	4.48	6.50	396
14	127.5	73.5	4.70	112	0.1632	54.0	0.02	0.02	0.19	—	4.49	6.91	524
15	127.5	73.3	4.70	112	0.1804	54.2	0.02	0.02	0.18	—	4.50	6.91	576
16	123.5	73.5	4.70	112	0.3080	50.0	0.02	0.02	0.14	—	4.54	7.75	988
17	126.0	73.5	4.70	112	0.2332	52.5	0.02	0.02	0.19	—	4.49	7.10	752
18	124.0	80.0	3.14	0	0	44.0	0.02	0.01	0.16	—	2.97	5.60	0
19	124.0	80.0	3.14	53	0.0584	44.0	0.02	0.01	0.16	—	2.97	5.60	88
20	123.0	80.0	3.14	53	0.0788	43.0	0.02	0.01	0.15	—	2.98	5.73	236
21	118.0	80.0	3.14	130	0.1508	38.0	0.02	0.01	0.13	—	3.00	6.57	560
22	114.0	80.0	3.14	130	0.2020	34.0	0.02	0.01	0.13	—	3.00	7.45	760
23	117.0	82.0	3.14	130	0.1604	37.0	0.02	0.01	0.13	—	3.00	6.76	612
24	110.0	80.0	3.20	130	0.2640	28.0	0.02	0.01	0.11	—	3.08	9.16	1208
25	149.3	76.0	6.26	0	0	73.3	0.02	0.02	0.28	—	5.96	6.60	0
26	148.1	75.8	6.26	130	0.0580	72.3	0.02	0.02	0.27	—	5.97	6.73	206
27	148.1	75.9	6.26	130	0.0800	72.4	0.02	0.02	0.27	—	5.97	6.73	284
28	147.0	75.6	6.27	130	0.1052	71.4	0.02	0.02	0.26	—	5.99	6.86	376
29	146.0	75.8	6.27	130	0.1216	70.2	0.02	0.02	0.26	—	5.99	6.98	436
30	145.5	75.9	6.30	130	0.1532	69.6	0.02	0.02	0.26	—	6.02	7.05	550

Vita

Lieutenant Robert M. Russ was born ███ ████████

███████████ He attended ██████████████████

██████████████ In 1956, he graduated from the Georgia

Institute of Technology with a degree in Aeronautical

Engineering. After working briefly for the Boeing Airplane

Company in Wichita, Kansas, he was called to active duty in

March of 1957. Upon completion of a maintenance officer

course at Chanute AFB he was assigned to duty with the

Strategic Air Command at Biggs AFB, Texas. Subsequently,

he entered resident training for Astronautical Engineering

(Graduate) at Wright-Patterson Air Force Base, Ohio.

Permanent address: ████████████████

████████████

This Thesis was typed by the author.